Theses and Dissertations   1. Thesis and Dissertation Collection, all items

1969-12

Design of an improved acoustic system for determination of the concentration of microbubbles in the ocean

Donaldson, William Jay; MacFarlane, Byron Noble

Monterey, California. Naval Postgraduate School

https://hdl.handle.net/10945/40129

United States
Naval Postgraduate School

THESIS

DESIGN OF AN IMPROVED ACOUSTIC SYSTEM FOR
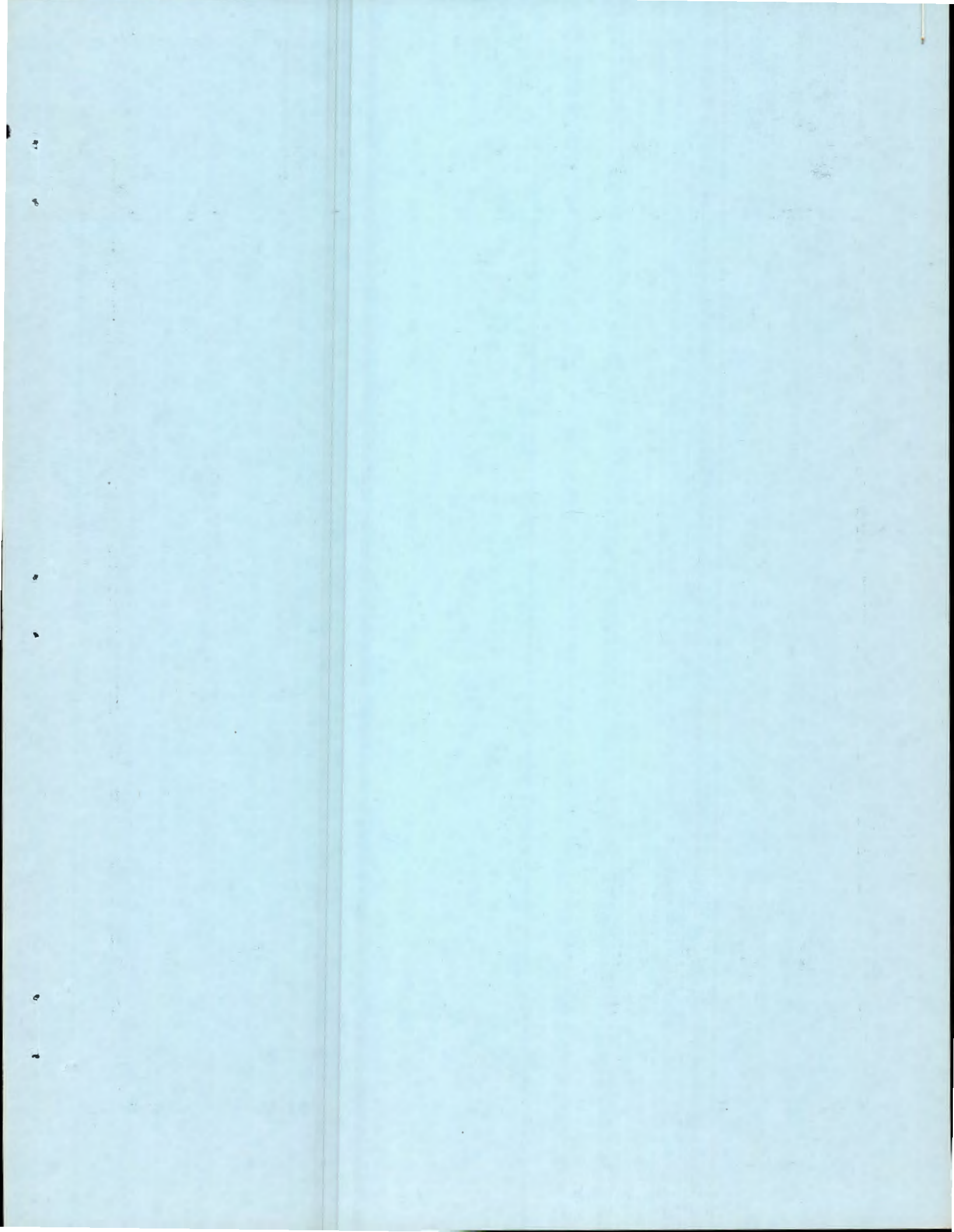DETERMINATION OF THE CONCENTRATION OF
MICROBUBBLES IN THE OCEAN

by

William Jay Donaldson
and
Byron Noble Macfarlane

December 1969

This document has been approved for public release and sale; its distribution is unlimited.

Design of an Improved Acoustic System for
Determination of the Concentration of
Microbubbles in the Ocean

by

William Jay Donaldson
Lieutenant, United States Navy
B.S.M.E., Purdue University, 1962

Submitted in partial fulfillment of the
requirements for the degree of
MASTER OF SCIENCE IN ELECTRICAL ENGINEERING

and

Byron Noble Macfarlane
Lieutenant Commander, United States Navy
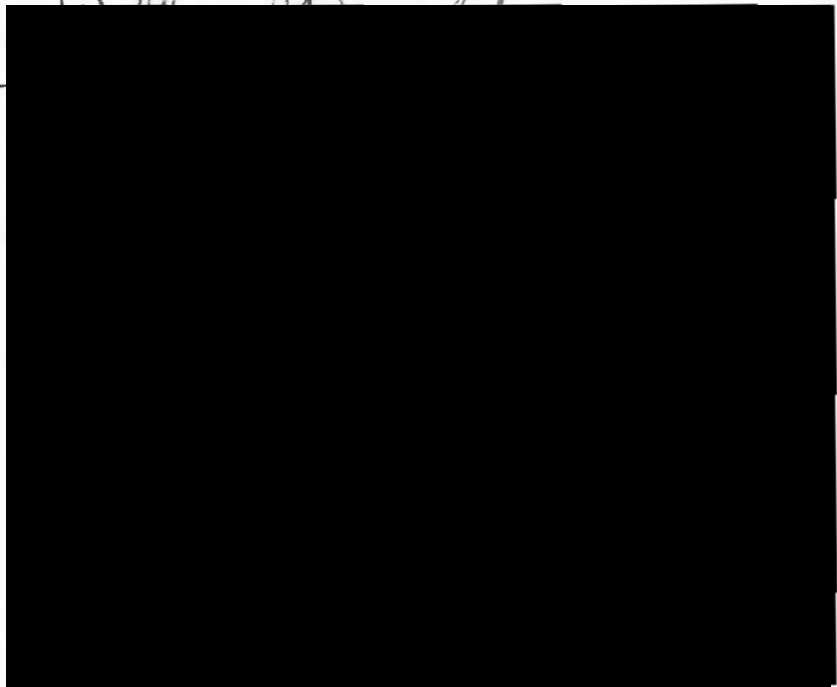B. S., United States Naval Academy, 1959

Submitted in partial fulfillment of the
requirements for the degree of
MASTER OF SCIENCE IN ENGINEERING ACOUSTICS

from the

NAVAL POSTGRADUATE SCHOOL
December 1969

Authors:

Approved by:

ABSTRACT

An acoustic system was designed to investigate microbubble concen-
trations and distributions in the ocean. The system consisted of a
one-dimensional standing-wave resonator and a reverberation sensor.
Concentrations are determined by measurement of the variation in
system Q and the change in reverberation level produced by the reso-
nant bubble response. The resonator and the sensor, while functioning
independently, both measure bubble concentration as a function of
depth and inferred size and thus provide a unique data comparison.
The system has been designed to measure bubbles from approximately
700 microns to 30 microns utilizing frequencies from 5 to 100 kHz at
depths to 100 ft. Initial tests utilizing a bubble generator in an
anechoic tank have demonstrated the system's capability to measure
bubble concentrations.

TABLE OF CONTENTS

4

LIST OF TABLES

LIST OF FIGURES

ACKNOWLEDGMENT

I. INTRODUCTION

In the summer of 1956 Blanchard and Woodcock rolled up their trousers, waded into the surf and collected the first in-situ information concerning bubble concentrations in the ocean. [1] Not to be outdone, Glotov, Kolobaev and Neuimain of the USSR generated breaking waves in a laboratory tank to provide bubbles for measurement in 1962. [2]

However crude these attempts may sound, they provided a substantial proportion of the data concerning bubble concentrations in the ocean until 1964 when, at the Naval Postgraduate School, work commenced on various projects to provide meaningful in-situ data concerning bubble concentrations in the ocean. [3,4,5] Concentrations of bubbles in the ocean have great effect on sound propagation in the sea through scattering and absorption. In addition, many oceanographic and meteorological phenomena can be attributed to them. Bubbles are created and distributed through the ocean by many different mechanisms. Obvious sources of bubbles include breaking waves, ships' wakes, plant and animal life. Internal waves and chemical changes are being investigated as other possible producers. The orbital motion of water particles due to wave action distributes bubbles in the upper layers of the ocean. In the ephotic zone, plant and animal life contribute to the distribution. Bubbles traversing to the surface are collectors of particulate matter; consequently, they affect the chemistry of the ocean, provide cavitation nuclei, and upon bursting at the surface produce airborne salt nuclei which can be linked to thunderstorm activity. [1] Therefore, a thorough knowledge of ocean bubbles is vital for the scientist and engineer working in the ocean environment.

11

To alleviate problems encountered in previous measuring techniques, an improved system for bubble concentration measurement was developed. This system consisted of a one-dimensional standing-wave resonator and a reverberation sensor. The resonator and the sensor, while functioning independently, both measure bubble concentrations as a function of bubble depth and size and thus provide a unique data comparison. The system has been designed to measure bubbles from approximately 700 microns to 30 microns utilizing frequencies from 5 to 100 kHz at depths to 100 feet.

II. ACOUSTIC THEORY OF BUBBLES

The compressions and rarefactions of a sound wave, when incident on a gas bubble in the ocean, cause the bubble to expand and contract. A portion of the energy transferred to the bubble is reradiated as scattered sound and the remainder dissipated in the oscillations. The ratio of the energy lost from the sound wave to the intensity incident on the bubble is defined as the extinction cross section, σ_e. The extinction cross section is comprised of the absorption cross section, σ_a, and the scattering cross section, σ_s, which are related to the absorbed and scattered energy of the sound wave.

The amplitude of the oscillation of the bubble depends on the size of the bubble and the frequency of the incident sound wave. At a specified frequency and corresponding bubble size, a resonant response occurs and the energy transferred from the sound wave is maximum. It can be shown that 75% of the energy lost by the sound wave is due to bubbles of radii that are within 10% of the resonant radius. [4]

The resonant frequency of a clean bubble, f_0, is [6]

$$f_0 = \sqrt{\frac{1}{2\pi a} \frac{3\gamma P_0}{\rho}}$$

where

$$f_0 = \text{resonant frequency, Hz}$$

$$\rho = \text{density of water, gm/cm}^3$$

$$a = \text{bubble radius, cm}$$

$$\gamma = \text{ratio of specific heats of bubble gas}$$

$$P_0 = \text{hydrostatic pressure, dynes/cm}^2$$

It therefore follows that, for air bubbles,

13

$$f_o = \frac{3.26 \times 10^6}{a} \sqrt{1 + 0.097d}$$

where d = depth, m

           a = bubble radius, microns, Fig 1.

The extinction cross section per bubble is [6]

$$\sigma_e = \frac{4\pi a^2 \delta / ka}{\left(\left(\frac{f_o}{f}\right)^2 - 1\right)^2 + \delta^2} \tag{II-1}$$

where σ_e = extinction cross section, m^2

           δ = damping constant, a parameter of bubble dynamics which includes thermal, radiation and viscous effects, Fig 2. [7]

           a = bubble radius, m

           k = $2\pi/\lambda$, m^{-1}

           λ = wavelength, m

The resonant extinction cross section is

$$\sigma_{e_o} = \frac{2ac}{f_o}$$

where σ_{e_o} = resonant extinction cross section, m^2

           c = velocity of sound in water, m/sec

           f_o = resonant frequency, Hz

The resonant extinction cross section for a clean 10-kHz air bubble at a depth of 10 meters is 25.4 cm^2 and for 100 kHz is 0.115 cm^2. These values represent an extinction to geometrical cross section ratio of approximately 3800 at 10 kHz and 1700 at 100 kHz.

14

The scattering cross section per bubble, σ_s , is [6]

$$\sigma_s = \frac{4\pi a^2}{((\frac{f_o}{f})^2 - 1)^2 + \delta^2}$$

and at the frequency of resonance σ_s becomes

$$\sigma_{s_o} = \frac{4\pi a^2}{\delta^2}$$

Three assumptions have been made in the previous sections: First, that the particulate or organic matter on the bubble surface does not contribute to the extinction cross section, second, that the gas in the bubble is air, and third, that the extinction cross section is due solely to bubbles of resonant size. These assumptions and the relationships developed in this section are discussed by Medwin [8] and provide the background for further development of the specific theory necessary for the standing-wave and reverberation sections of the microbubble measurement system.

III. STANDING-WAVE SUBSYSTEM

A. THEORY

A standing wave can be established between two rigid reflectors for a series of allowed frequencies or modes of vibration. These NORMAL MODES of vibration are related to the spacing between the reflectors such that a resonant response occurs when the spacing is equal to multiples of a half wavelength. As in any resonant system, the standing wave can be described in terms of the system "quality factor," Q, as [9]

$$Q = 2\pi \frac{\text{Energy stored}}{\text{Energy dissipated}}$$

or as [10]

$$Q = \frac{f_o}{\Delta f}$$

where f_o = resonant frequency, Hz

    Δf = half-power bandwidth, Hz

or finally as [8]

$$Q = \frac{\pi}{\alpha \lambda}$$

where α = spatial attenuation, nepers/m

    λ = wavelength of the resonant frequency, m

When bubbles are present in the standing wave system, sound energy will be lost to the oscillations of the bubble as previously discussed in Section II. This loss of energy will be evident as a lower system Q.

$$Q_1 = \frac{\pi}{\alpha_1 \lambda}$$

where the subscript 1 denotes measurement in bubble free water

16

or

$$\alpha_1 = \frac{\pi}{Q_1 \lambda}$$

Similarly

$$\alpha_2 = \frac{\pi}{Q_2 \lambda}$$

where the subscript 2 denotes measurement when bubbles are present. The increased attenuation due to the bubbles, A, is found by combining the above equations

$$A = \alpha_2 - \alpha_1$$

$$= \frac{\pi}{\lambda} \left(\frac{1}{Q_2} - \frac{1}{Q_1} \right)$$

$$= \frac{\pi}{\lambda f_0} (\Delta f_2 - \Delta f_1) \qquad \text{nepers/m}$$

$$= \frac{8.68\pi}{c} (\Delta f_2 - \Delta f_1) \qquad \text{dB/m} \qquad \text{(III-1)}$$

where c = velocity of propagation, m/sec.

The attenuation due to bubbles can be related to the extinction cross section, σ_e , [6] as defined in equation (II-1)

$$A = 4.34 n \sigma_e \qquad \text{dB/m}$$

where n = number of bubbles per cubic meter.
Correcting this equation for the volume between reflectors of the standing wave system gives

$$A = \left(\frac{4.34}{V} \right) n \sigma_e \qquad \text{dB/m} \qquad \text{(III-2)}$$

Combining equations (III-1), (III-2) and (II-1) provides the expression for the number of bubbles per cubic meter

17

$$A = (\frac{4.34}{V}) n\sigma_e = \frac{8.68\pi}{c} (\Delta f_2 - \Delta f_1)$$

$$n = \frac{2\pi V}{c\sigma_e} (\Delta f_2 - \Delta f_1)$$

$$n = \frac{V\pi f_0 (\Delta f_2 - \Delta f_1)}{c^2 a} \qquad \text{(III-3)}$$

B. PRELIMINARY INVESTIGATION

Previous investigators pointed out the many problems connected with the design of a standing-wave system utilizing a mylar transducer as one of the two reflectors. [4,5] With such a configuration, results were not consistent due to the variation of the transducer parameters with time and depth. A solution to this dilemma is to excite a standing-wave pattern between two reflectors with a loosely coupled external transducer. Such a system depends only on the characteristics of the reflectors and not on the parameters of the transducer. The ideal reflector is either a pressure-release surface or a rigid boundary. Since these surfaces can not be readily obtained, an optimum reflector must be chosen from materials available.

A rigid reflector implies that the material has a high characteristic impedance, such as steel. It has a pressure antinode established at its boundaries and therefore a sensor mounted in the reflector can be utilized for determination of the maximum pressure for all frequencies concerned. The utilization of this type material implies a massive system.

A pressure-release system, having low characteristic impedance, can be realized with a thin membrane backed by air or vacuum. This reflector

18

has a pressure minimum at the boundary and therefore as the frequency is changed, a pressure-measuring device must be shifted within the system in order to measure the pressure antinodes. Such a system would be light-weight and thus portable. Since an oceangoing device must be mobile, the pressure-release system was chosen for the initial development.

The first pressure-release reflector investigated was 1/2-inch polyethylene. This was chosen because of its previous use. [5] The reflector had been constructed by coating the polyethylene with neoprene and supporting it with a 22-inch-square, 1/2-inch-thick aluminum plate. To evaluate the performance of the reflector, standing wave measurements were taken. The reflector was illuminated with a mylar transducer and the resulting standing-wave ratio measured. The polyethylene was an extremely poor performer in that SWR varied between 3.4 to 14 (Q ranging between 5.4 and 22) in the frequency range of 10 to 100 kHz.

The second reflector tested was a neoprene-coated 1/2-mil mylar surface stretched across a 1-inch-thick fiber honeycomb. This combination was also backed with a 22-inch-square, 1/2-inch-thick aluminum plate for rigidity. [5] This system was so tender that the tests were never completed due to numerous leaks.

The complications listed above led to the construction of an aluminum-bounded fiber honeycomb reflector. The reflector consisted of 2-inch-thick fiber honeycomb laminated between two 0.060-inch aluminum plates. This reflector provided a SWR which varied between 4 and 15 in the frequency range of 10 to 100 kHz.

In an attempt to eliminate transmission through the interior of the reflector, a vacuum reflector was constructed from 0.012-inch aluminum

19

plates and 0.005-inch aluminum foil honeycomb. When evaculated to seventeen inches of mercury, there was still significant variation of SWR with frequency similar in magnitude to the preceeding reflector, indicating that energy was still being transmitted through the honeycomb.

A system was constructed of two aluminum-bounded fiber honeycomb reflectors spaced six inches apart for a 5-kHz fundamental resonance. An external 7 by 91 centimeter rectangular mylar-slat transducer was used to excite the system. [5] No evidence of standing waves inside the system was observed with the use of either the slat transducer mentioned above or a 25-centimeter circular mylar transducer.

It was apparent at this time that in spite of the weight advantages of the pressure-release concept, it would provide an unsatisfactory resonant standing-wave system due to the variation of reflectivity with frequency and the necessity for changing the probe to measure the pressures within the system.

Attention was next shifted to the rigid reflector. Although light in weight, aluminum was rejected due to its low characteristic impedance which would produce a theoretical reflectivity of 0.84. Thus, although heavy, steel with a characteristic impedance of 47×10^6 MKS Rayls and a theoretical reflectivity of 0.94 was selected. Two square steel plates (2 by 2 feet) were cut to form the boundaries of the system. The slat transducer, Fig 3, failed to provide enough energy when used external to the system and was too bulky to utilize internally. The system was excited with the 25-centimeter circular mylar transducer. As the tests proceeded the plates were cut to a circular shape to provide a more efficient energy cavity. A 15-cm spacing was utilized. The dimensional stability was established by bolting the plates together with four, 6-inch, threaded 1/4-inch studs. No identifiable 5-kHz resonances were observed,

but distinct peaks were present at intervals of approximately 300 Hz.
A natural resonant mode of the plates was found at 231 Hz for one plate
and 232 Hz for the other. Therefore it was apparent that the ringing
of the plates affected the establishment of the standing-wave system.
The plates were isolated with rubber bushings and rubber washers, but
no appreciable change in system performance was noted. To eliminate
the natural resonance of the plate a polyester resin, thirty-mesh sand
mixture was applied to the back of one plate to a depth of approxi-
mately four centimeters. The second plate was damped with the conical-
design ρc rubber. This damping eliminated the 300-Hz ringing of the
plates. To increase the energy input of the system a barium titanate
transducer was constructed; the response of this transducer was disap-
pointing as the effective frequency range was only 75 to 100 kHz. A
second transducer was constructed with a different design, its frequency
range was from 11 to 100 kHz. The internal resonances of the transducer
provided a sound-pressure level far from the flat response obtained
through the use of a mylar transducer.

The system still did not produce a standing wave. It appeared at
this point that the warpage in the plates, which had been noted and con-
sidered small, was causing interference effects which were prohibitive
to the establishment of a standing wave in the resonant cavity. The
plates were spaced by the holding studs at 152($\pm$2) mm; however the
interior of the system bulged as much as 7 mm. Reflectivity tests were
conducted on the polyester-sand damped plate. The results presented in
Fig 4 showed a reflectivity close to unity for frequencies 20-100 kHz
except for dips at approximately 36 and 72 kHz. This effect can be
attributed to a standing wave being established in the damping material
itself. Theory predicts that transmission through a material will occur

21

at frequencies which are multiple half wavelengths. These frequencies, f_n, are:

$$f_n = \frac{nc}{2\ell}$$

where   n = integers 1,2,3, ...

             c = velocity of sound in material, m/sec

             ℓ = thickness of material, m

If the c of the resin-sand mixture was 2900 m/sec, which is reasonable, then a standing wave will be produced in the damping material at frequencies of 36 and 72 kHz. To correct this deficiency the application and type of damping material must receive further consideration.

A third barium titanate transducer was constructed and tested. The frequency response from 10 to 50 kHz was very poor and the transducer did not become effective until 200 kHz. With the disappointing frequency response of the three barium titanate transducers it was decided that mylar offered by far the most advantages.

A standing wave was established between the mylar transducer and the polyester-sand damped steel plate. The Q of the system was dependent on the spacing between the reflectors. The optimum spacing for this resonator was noted as 54 cm for frequencies of 30 and 68 kHz, Fig 5. The optimization of spacing is presumably due to a balance between loss per meter at reflection, which decreases with larger separation, and loss due to divergence of the near-plane wave which increases with larger separation.

C. FINAL DESIGN

The optimum system would consist of two steel plates of infinite extent and infinite thickness. Considering the weight of steel (10 pounds

per ft^2 for 1/4-inch plate) the size must be limited. A compromise decided upon was a circular steel plate of 2 1/2 ft diameter (weight about 50 lbs) to insure that the total section, including damping material and associated equipment could be handled aboard a small ship. The steel plates are spaced as determined in the calibration, Section VI. This spacing provides resonant frequencies of approximately 1 to 2 kHz and multiples thereof through the range from 10 to 100 kHz.

Investigation into the optimum damping material revealed that the Navy is presently utilizing an epoxy-sand mixture to damp steel plates in and around the sonar domes of the new-construction DE 1052-class Destroyers. [11] It was decided to use the same technique to damp the standing-wave-section steel plates. To insure that a standing wave was not again established in the backing, the epoxy-sand mixture was formed into a lattice of variable-impedance transition tetrahedrons, Fig 6. Based on past experience with variable-impedance transition, the tetra-hedrons were chosen to be 1 1/4 inches high with a vertex angle of 30 degrees. The backing was constructed by casting APCO 210 epoxy and 30-mesh sand (1 part epoxy to 4 parts sand by weight). The epoxy-sand mixture was cast in a flexible RTV 630 silicone-rubber mold made from a 1/4-circle wood master, Fig 6. The molding of the backing proved to be a long and tedious process.

The mylar transducer was mounted directly on the face of one of the steel plates. The steel plate was used as one electrical contact surface and an annular ring of mylar 10-cm wide completed the active surface, Fig 7.

A 1/2-inch-long, 1/4-inch-diameter barium-titanate probe was utilized as a pickup. [5] The probe was small enough not to disturb the sound field and large enough to provide a satisfactory output. A preamplifier

23

was utilized at the hydrophone to present a high impedance to the barium titanate and to reduce the noise in the system. The pickup was mounted in the center of the steel plate already containing the mylar transducer to insure that the acoustic intensity received by the probe was due principally to the standing wave established in the system rather than the direct transducer radiation. The electronics associated with the section are shown in Fig 8 and Table 2.

IV. REVERBERATION SUBSYSTEM

A. THEORY

The mechanism of absorption and scattering by bubbles has been previously discussed in Section II. The total omnidirectional scattering cross section per unit volume can be defined as follows:

$$\sigma_{st} = 4\pi \frac{I_{scat}}{I_{inc}}$$

where

I_{scat} = scattered intensity at unit distance produced by ensonified volume

I_{inc} = incident intensity on ensonified volume.

The concentration of bubbles in a known ensonified volume can be obtained by measuring the total scattering cross section of the volume, calculating the scattering cross section of a single bubble and computing the ratio of the two quantities, assuming no interaction between bubbles.

Figure 9 will be helpful in understanding the theoretical development for the measurement of total scattering cross section and hence the concentration of bubbles in a volume. Utilizing standard spreading loss relationships to solve for I_{inc} and I_{scat}

$$I_{inc} = \frac{4\pi(1)^2}{4\pi r^2} I_o$$

$$= \frac{I_o}{r^2}$$

where

I_o = source intensity (at 1 meter)

25

and

$$I_{rec} = \frac{4\pi(1)^2}{4\pi r^2} I_{scat}$$

$$= \frac{I_{scat}}{r^2} \quad .$$

Rearranging,

$$I_{scat} = I_{rec} r^2 \qquad [12]$$

Substituting the measurable intensities, I_o and I_{rec}, into the definition for total scattering cross section gives

$$\sigma_{st} = 4\pi \frac{I_{rec}}{I_o} r^4 \quad .$$

This expression for σ_{st} must now be corrected for the volume ensonified, V,

$$V = \frac{c\tau}{2} \psi r^2$$

where   V = volume, m^3
          c = velocity of sound, m/sec
          τ = signal pulse length, sec
          ψ = solid angle ensonified
          r = range, m

Therefore

$$\sigma_{st} = \frac{4\pi \; I_{rec} \; r^4}{I_o \; \frac{c\tau}{2} \; \psi r^2} \quad .$$

Cancelling and rearranging

$$\sigma_{st} = \frac{8\pi \; I_{rec} \; r^2}{I_o \; c\tau\psi} \qquad\qquad (IV-1)$$

The scattering cross section of a single resonant bubble, σ_{s_o} , is

$$\sigma_{s_o} = \frac{4\pi a^2}{\delta^2}$$ (IV-2)

where a = bubble radius, m

δ = damping constant .

The number of bubbles of resonant radius present in a volume of one cubic meter, n , is

$$n = \frac{\sigma_{st}}{\sigma_{s_o}}$$. (IV-3)

Substitution of equations (IV-1) and (IV-2) into equation (IV-3) yields

$$n = \frac{2}{c\tau\psi} \left(\frac{r\delta}{a} \right)^2 \frac{I_{rec}}{I_o}$$. (IV-4)

B.   DESIGN

A 60-cm-diameter electrostatic mylar transducer was selected for the reverberation subsystem. The transducer, through the use of a TR switch, Appendix B, was utilized in both transmit and receive modes. The large size was selected to provide adequate output power and sensitivity for reception particularly of the low-frequency backscattered sound. The transducer was oriented to provide normal incidence with the surface of the ocean. The time of reflection from the surface is the depth reference for the entire system. The electronics associated with the section are shown in Fig 10 and Table 3.

V. PROPOSED COMPOSITE SYSTEM DESIGN

To form a composite system the standing-wave and reverberation sections should be mounted in a rigid frame. The frame would be constructed in the form of a 3 1/4-ft cube with positive buoyancy provided by 5 ft^3 of styrofoam. Details of the proposed construction are illustrated in Fig 11.

Two pressure-proof containers were constructed, one for each subsystem from 2 7/8-in-diameter copper pipe, Fig 12. The standing-wave container housed a single preamplifier and the reverberation container held two preamplifiers and the TR switch, Fig 13.

In order to maintain the composite system at a predetermined depth a controllable anchoring device was designed. The device is operable from the surface, provides positive control of depth and is simple enough to insure a high degree of reliability. Specific design details are illustrated in Fig 11.

VI. CALIBRATION

A. DISCUSSION

To solve the equations for bubble concentration, both standing-wave and reverberation subsystem characteristics must be measured. Once these characteristics are known, the system can then be utilized. To insure the validity of the measurement theory and that the proper characteristics of the system have been obtained, bubbles of known size and concentration should be generated for measurement.

B. STANDING-WAVE SUBSYSTEM

The annular mylar transducer operated satisfactorily for 5 minutes during the initial test. The transducer was rebuilt and subsequently failed for a second time after 10 minutes of operation. The output of the transducer appeared to be greater than that of the 25-cm mylar transducer; however no measurements were obtained. The failures of the annular mylar transducer required that the subsystem calibration be conducted utilizing the standing-wave subsystem 2 1/2-ft-diameter steel plate as one reflector and the 25-cm mylar transducer as the other reflector and source. The Q of the standing-wave subsystem was measured at 27.5 kHz and 76 kHz while varying the spacing between the transducer and reflector plates, Fig 14. The maximum Q of 380 at 76 kHz obtained with the variable impedance transition backed steel plate (45 cm spacing) is three times as large as the optimum obtained with the 2-ft-diameter resin-sand backed steel plate at 68 kHz (54 cm spacing), Fig 5. The Q of 380 represents a reflectivity of 0.99 which indicates that the elimination of plate warpage and application of the variable-impedance

transition backing has corrected the reduced reflectivity observed between 63 and 80 kHz in Fig 4. A previous Pulse-Echo System [4] with a 1-ft-diameter steel plate, which has been used at sea, produced a Q of 150 at 76 kHz. With the standing wave system fixed at 45 cm, a complete sweep of the frequency range was made, utilizing the B&K Model 2304 Level Recorder as a recorder, to establish the bubble-free half-power bandwidth, Δf_1. A section of this sweep is shown in Fig 15.

The bubble generator, Appendix C, was used to provide bubble concentrations of 300 ($\pm$200) bubbles/m^3 of 125 ($\pm$10) microns radius while operating at a depth of 1.5 m. With these bubbles present the measured system Q was 62 corresponding to a half-power bandwidth of 420 Hz at a resonant frequency of 25,956 Hz. Utilizing equation III-3 the concentration of bubbles was calculated as approximately 100 bubbles/m^3 of 130 ($\pm$8) microns radius.

C. REVERBERATION SUBSYSTEM

The solid angle of ensonification, ψ , of the 60-cm-diameter mylar transducer is obtained by measuring the directivity pattern of the transducer, plotting the angle between the half-power points, θ_{3dB}, and solving the equation for the solid angle:

$$\psi = 2\pi \left(1 - \cos \frac{\theta_{3dB}}{2}\right) \qquad 0° \leq \theta_{3dB} \leq 180°$$

A typical directivity pattern, taken at 20 kHz, is shown in Fig 16. A plot of θ_{3dB} versus frequency, taken from the directivity patterns is shown in Fig 17. A plot of ψ versus frequency is shown in Fig 18.

The transducer pressure level, Fig 19, and the receiving sensitivity level, Fig 20, were measured in order to calculate the output and received intensities. To monitor the output intensity of the system when

30

it is utilized at sea a 1/4-inch barium-titanate probe is provided adjacent to the transducer. A plot of monitor probe voltage versus transducer SPL would provide the necessary data for the probe's utilization.

The bubble generator, Appendix C, was used to provide bubble concentrations of 650 ($\pm$250) bubbles/m^3 of 120 ($\pm$15) microns radius. With these bubbles present the received to output intensity ratio was 2×10^{-3}. The received echo represents the minimum detectable signal which could be distinguished from the noise. Utilizing equation IV-4 the concentration of bubbles was calculated as approximately 500 bubbles/m^3 of 130 ($\pm$8) microns radius at a resonant frequency of 26 kHz.

VII. DATA HANDLING

A. DISCUSSION

To facilitate data reduction, automated data handling should be utilized. Data reduction would be accomplished as follows. Output data from the composite system are collected by a multiple-channel tape recorder. This analog is converted by the hybrid COMCOR CI 5000/ SDS 9300 computer to digital format. The IBM 360 computer processes the digital information and produces the following:

   (1) A plot of bubble concentration, n, versus bubble radius, a, at specified depths.

   (2) A plot of bubble concentration, n, versus bubble depth, d, at specified radii.

Each section of the composite system will produce data independently. These data are then presented on a composite plot.

B. STANDING-WAVE SUBSYSTEM

Figures 21 and 22 illustrate the flow of data in the standing-wave subsystem. The input data in analog form, i.e., Q curve, is transformed to digital format, normalized and plotted as one output of the computer program. Half-power bandwidth, f_1, and center frequency, f_0, of the Q curve are combined with quantities determined through solution of auxiliary equations to solve the relation for bubble concentration as developed in Section III. These auxiliary equations are:

$$f_2 = \text{half-power bandwidth, bubble-free water, for specific resonant frequencies}$$

$$\delta = 2.14 \times 10^3 \, f_0^{0.35} \text{ (fitted to Devin [7] for } 10^4 < f_0 < 10^5)$$

$$c = 1449 + 4.6T - 0.05T^2 + 0.0003T^3 + 0.017d$$

$$a = \frac{3.26 \times 10^6}{f_0} \sqrt{1 + 0.97d}$$

$$d = \frac{ct_{max}}{2} + .6 \quad \text{or data card input}$$

where δ = damping constant

t = time for return of surface reflection (from reverberation section, sec)

c = speed of sound, m/sec

T = temperature of the water, C

a = bubble radius, microns

f_0 = frequency, Hz

d = depth of bubble concentration, m, (in this case standing-wave-section depth). This depth is determined by the reverberation section and corrected to the center of the standing-wave section.

At a particular depth each resonant frequency will be swept 5 times to insure data accuracy. The depth of the section is varied and the data stored to provide the output plots.

C. REVERBERATION SUBSYSTEM

Figures 23 and 24 illustrate the flow of data in the reverberation subsystem. The basic technique is similar to the previous method of solution, but in this case the analog data takes the form of voltage, V, versus time, t_n , and is not normalized. The previous auxiliary equations are again utilized along with the following additions:

P_0 = pressure representation of the outgoing transducer intensity

$$d = \frac{c(t_{max}-t_n)}{2}$$

$$r = \frac{ct_n}{2}$$

$$\psi = 5.31 \times 10^6 \, f_0^{-1.94}$$

33

where   d   = depth of bubbles, m

           r   = distance from transducer to bubbles, m

           ψ   = solid angle ensonified

At a particular depth specified frequencies will be pulsed 5 times to
insure data accuracy. The return reverberation provides a measure of
bubble concentration over a range of depth. Bubble size is determined
by utilizing various frequencies. The composite plot can now be con-
structed from the standing-wave and reverberation subsystem data.

VIII. <u>CONCLUSIONS</u>

A. DISCUSSION

Initial tests utilizing the bubble generator, Appendix C, in the anechoic tank demonstrated the composite system's capability to measure bubble concentrations. The bubble size and concentration measured by the subsystems agreed within an order of magnitude.

B. STANDING-WAVE SUBSYSTEM

1. The pressure-release reflector concept could not be realized in practice. The internal strength members necessary to withstand external sea pressure and maintain dimensional stability provide a path of energy transmission through the reflector.

2. The rigid reflector must be a planar surface within a small fraction of a wavelength at the highest frequency utilized and the natural resonances of the reflector must be damped.

3. The damping material must be formed to provide variable-impedance transition and have a characteristic impedance between that of water and the reflector material.

4. The transducer must be mounted in the reflector face.

5. The transducer must be properly shielded to insure minimum direct electrical radiation.

6. The reflectors must be parallel to provide maximum system Q.

C. REVERBERATION SUBSYSTEM

1. To measure bubble concentrations less than 500 bubbles/m^3, the present signal-to-noise ratio must be improved.

2. The transducer must be properly shielded to insure minimum direct electrical radiation.

35

D. RECOMMENDATIONS

1. Construct a precision bubble generator which will provide bubbles of a uniform size and concentration for absolute calibration of the system.

2. Provide a means of measuring the bubbles in the anechoic tank while they are being generated for calibration, such as an underwater periscope.

3. After numerous failures of the annular mylar transducer the construction techniques were still not perfected and further investigation of the transducer should be conducted.

APPENDIX A

ALTERNATING-POLARIZATION SYSTEM

Investigations conducted on mylar transducers have shown that there is a change of output characteristics as a function of time. [4] After 24 hours of polarization the output characteristics stabilize. The stabilized output is much less than the initial output. [5] This variation is attributed to the slow polarization of the mylar film due to the applied D.C. voltage. A polarizing network was designed which would alternately apply positive and negative polarizing voltages to the mylar transducer.

The network, Fig 25, consisted of two silicon control rectifiers alternately triggered by a center-tap transformer. The circuit was designed to operate between 5 and 50 Hz; however redesign for a different frequency range could be accomplished through judicious choice of loading resistors. The network, in conjunction with unit pulse generators and function generators, provided a pulsed output signal superimposed on the positive peak of the polarizing voltage, Fig 26 and Table 4. Figure 27 is an oscilloscope picture of the system in operation.

APPENDIX B
TRANSMIT-RECEIVE NETWORK

In order to utilize the excellent sensitivity of the reverberation-section mylar transducer in both receive and transmit modes, a TR system, Fig 27 and Table 5, was developed. Several special-purpose TR systems had been designed by previous thesis students; however, none of these were suitable for use submerged at sea. The TR switch, Fig 13 and 29, was designed as a general-purpose circuit using a combination of a diode gate and an FET transistor to provide a lightweight and compact system utilizing minimum external power and controls. Figure 30 is an oscilloscope picture of the network in operation.

APPENDIX C

BUBBLE GENERATOR

To perform the final calibration and check the operation of the composite system a bubble generator was developed. [3] The generator was designed to provide bubbles which were resonant at a frequency midway in the spectrum of interest.

Electrolysis provided the method for generation of the bubbles. The bubbles were formed on Tungsten electrodes. Tungsten was selected as it was readily available and it would not participate in the electrolysis. The generator configuration is illustrated in Fig 31. It can be shown that bubble size is determined from: [13]

$$a = \sqrt{\frac{9 \, v \, \eta}{2g \, (\rho_w - \rho_a)}}$$

where

a = bubble radius, cm

η = dynamic shear viscosity, poise

v = bubble velocity, cm/sec

g = acceleration of gravity, cm/sec^2

ρ_w = density of water, gm/cm^3

ρ_a = density of air, gm/cm^3

FIGURE 1. BUBBLE RADIUS AS A FUNCTION OF RESONANT FREQUENCY AND DEPTH FOR AIR-FILLED BUBBLES
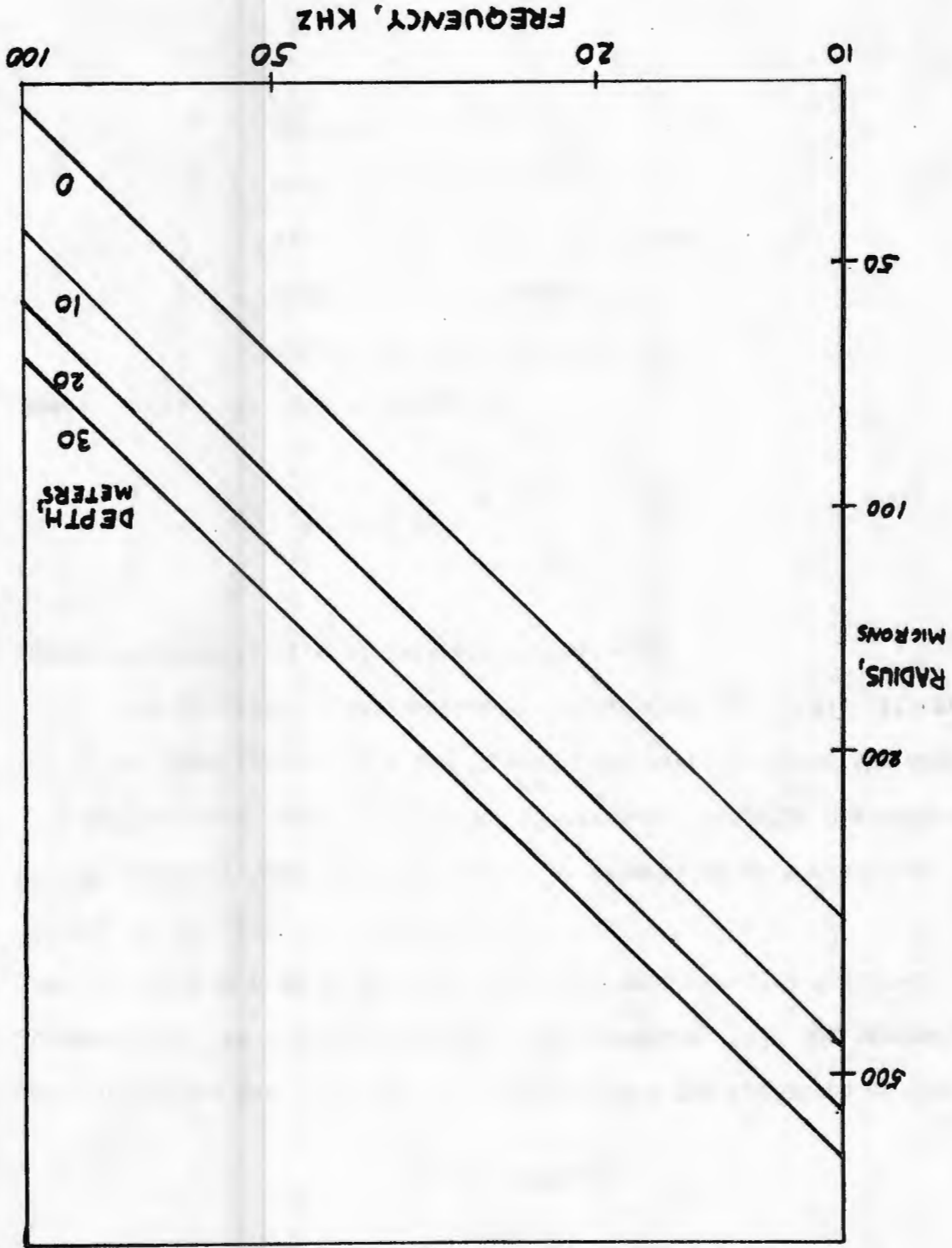
FIGURE 2. DAMPING CONSTANT AS A
FUNCTION OF FREQUENCY [7]

FREQUENCY, KHZ

DAMPING
CONSTANT

.02

.05

.1

.2

10

20

50

100
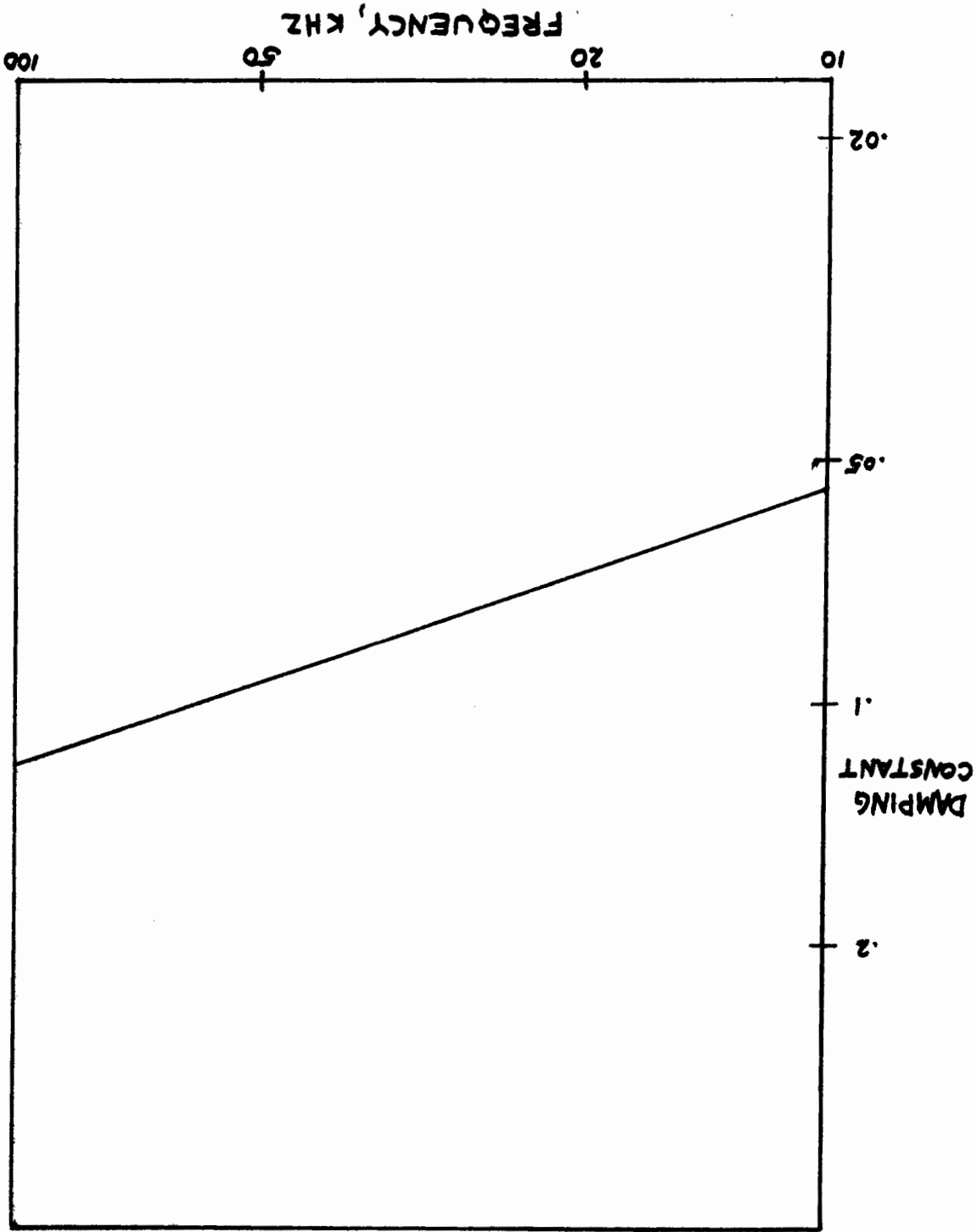
FIGURE 3. MYLAR-SLAT TRANSDUCER
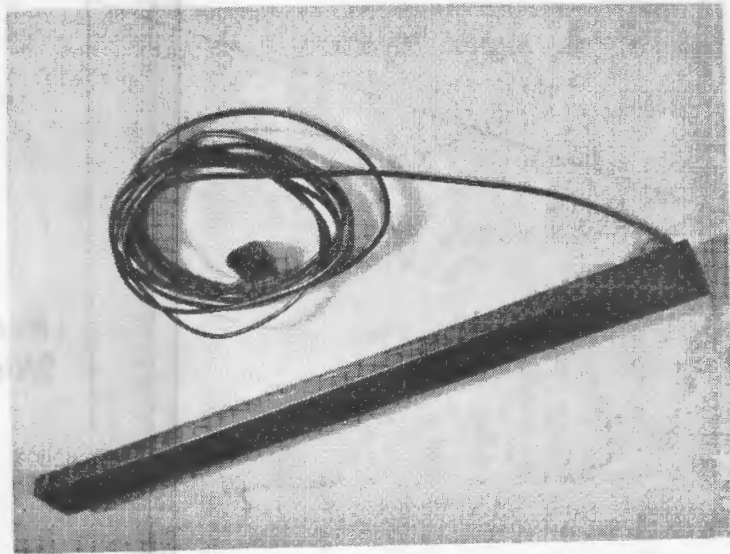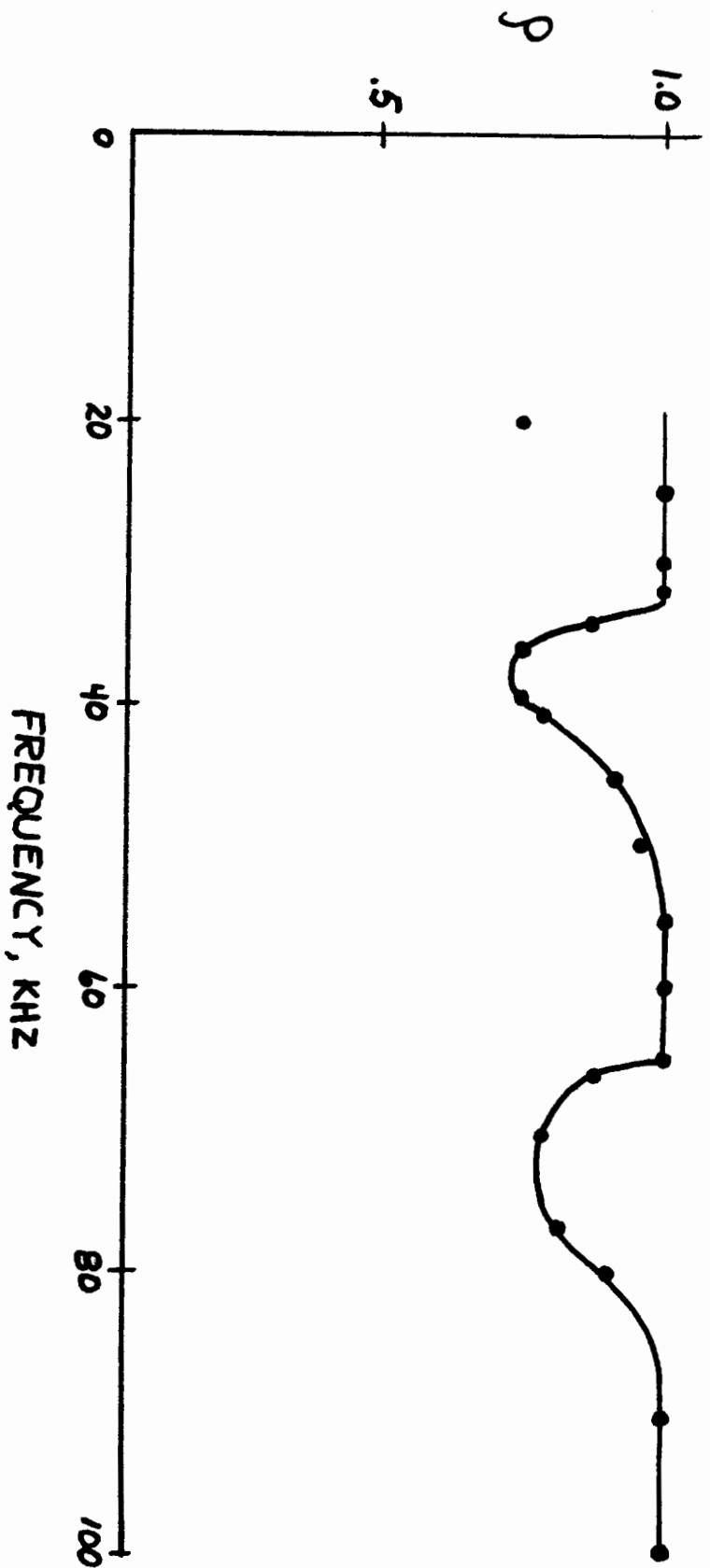
FIGURE 4. REFLECTIVITY OF RESIN/SAND-BACKED STEEL PLATE
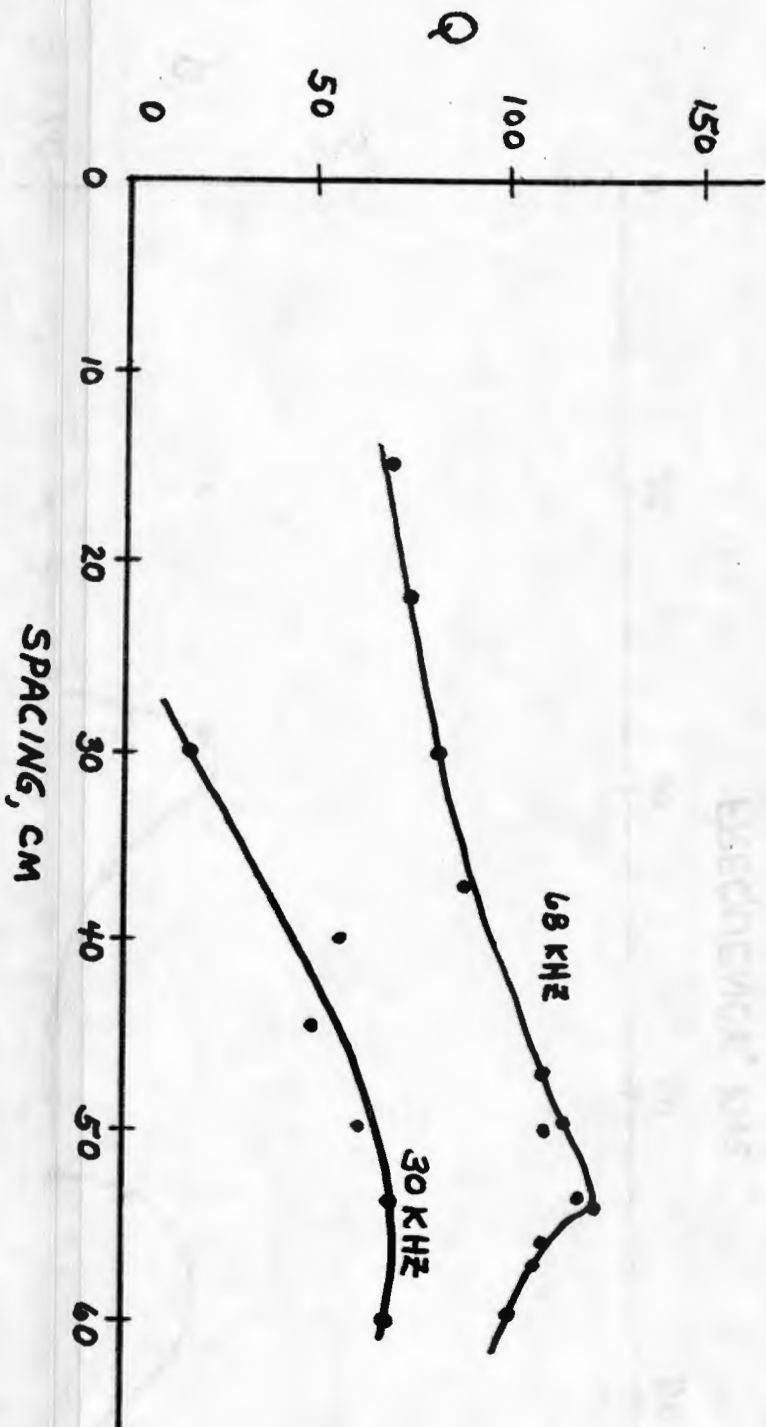
FIGURE 5. Q AS A FUNCTION OF SPACING AND FREQUENCY

SPACING, CM

Q

68 KHZ

30 KHZ
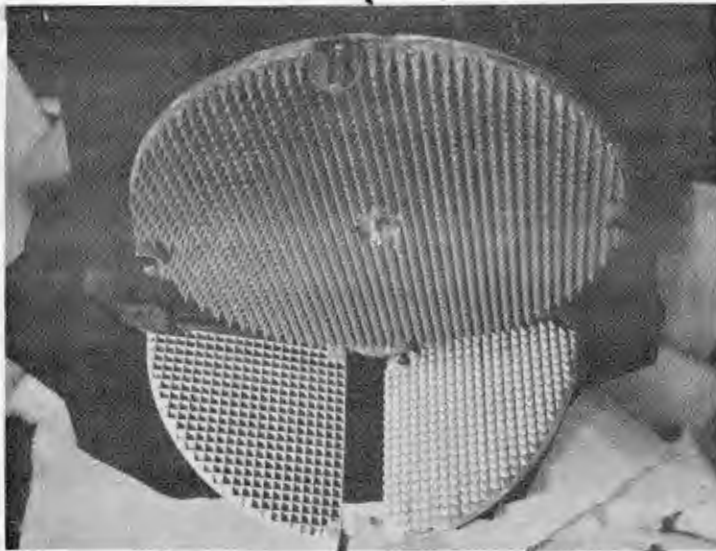
TABLE 1

STANDING-WAVE SUBSYSTEM TRANSDUCER DETAILS

Plate diameter	30	inches
Plate thickness	1/4	inch
Annular transducer o.d.	26	inches
Annular transducer i.d.	18	inches
Insulator groove depth	1/16	inch
Insulator groove width	1/2	inch
Pickup access diameter	1/2	inch
Tetrahedron backing thickness	1 1/4	inch

Note: plates ground flat, ± 0.005 inch.
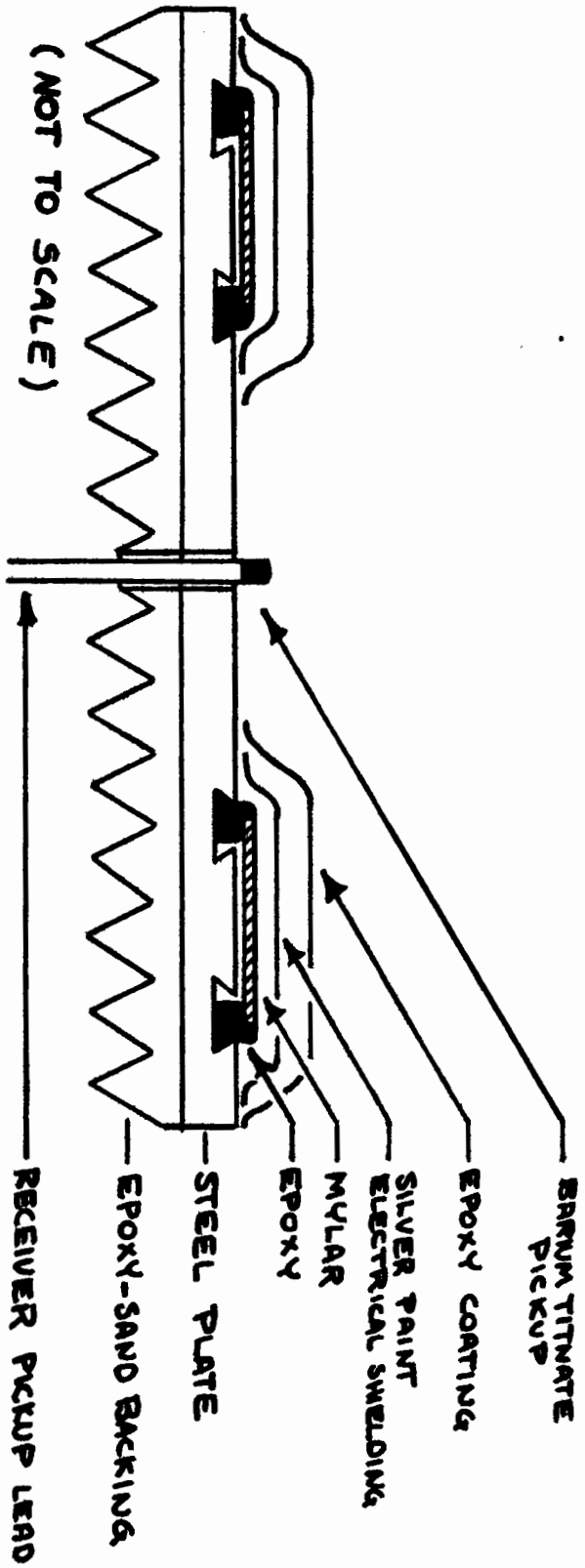
FIGURE 7. STANDING-WAVE SUBSYSTEM TRANSDUCER DETAILS

(NOT TO SCALE)

BARIUM TITNATE PICKUP

EPOXY COATING

SILVER PAINT
ELECTRICAL SHIELDING

MYLAR

EPOXY

STEEL PLATE

EPOXY-SAND BACKING

RECEIVER PICKUP LEAD

TABLE 2

STANDING-WAVE SUBSYSTEM COMPONENTS

Function Generator: Hewlett Packard 3300A Function Generator

Tone Burst Accessory: Hewlett Packard 3302A

Power Amplifiers: Hewlett Packard 467A Power Amplifier

Oscilloscope: Tektronix Type 545 Oscilloscope

Amplifier: Hewlett Packard 466A AC Amplifier

Preamplifier: NUS Model 2010-30 (30 dB gain)

Transducer: 10 cm Annular Mylar Transducer

Receiver: 1/4-inch Barium Titanate Pickup

Polarizer: Appendix C
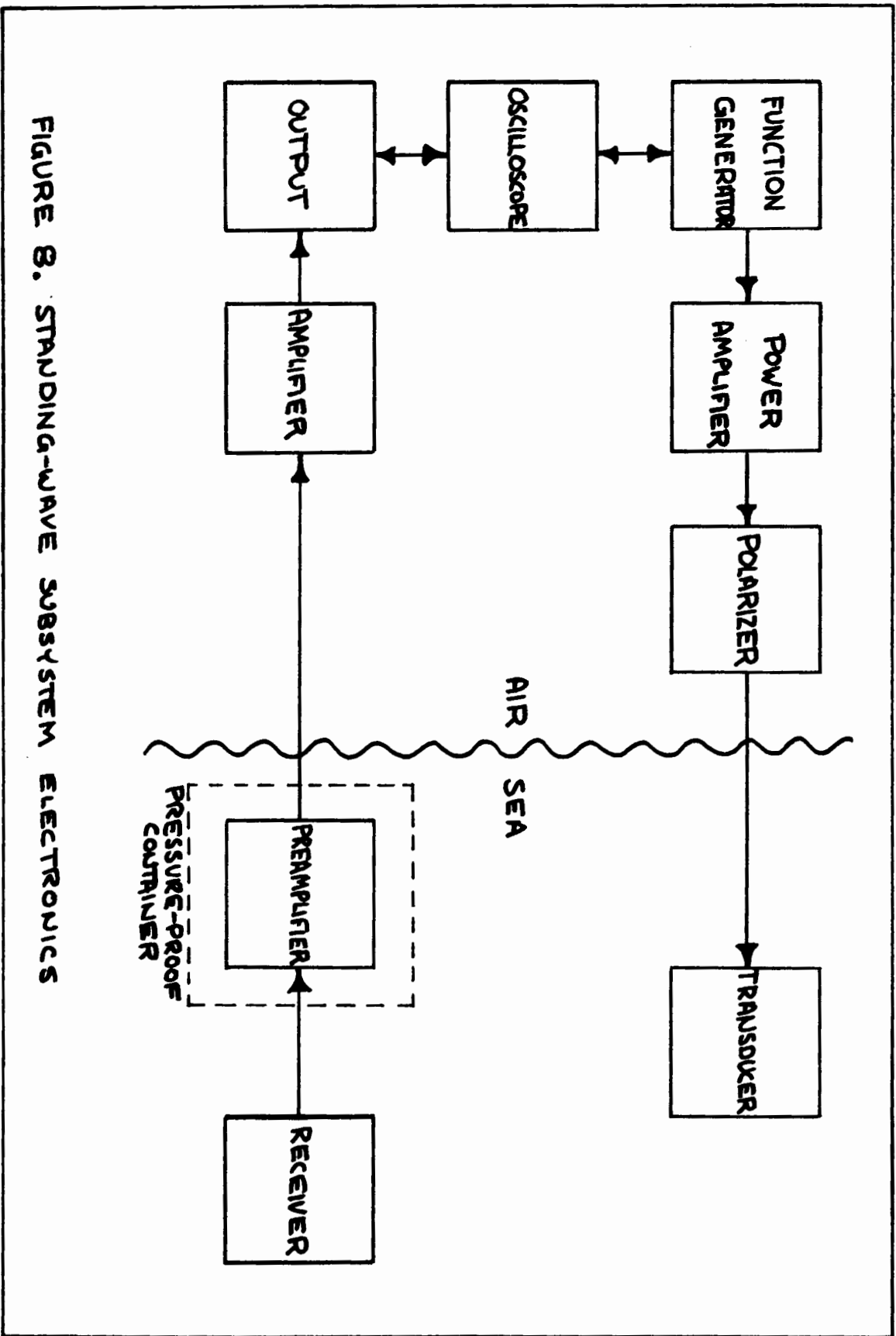
FIGURE 8. STANDING-WAVE SUBSYSTEM ELECTRONICS

FIGURE 9. REVERBERATION CONCEPT
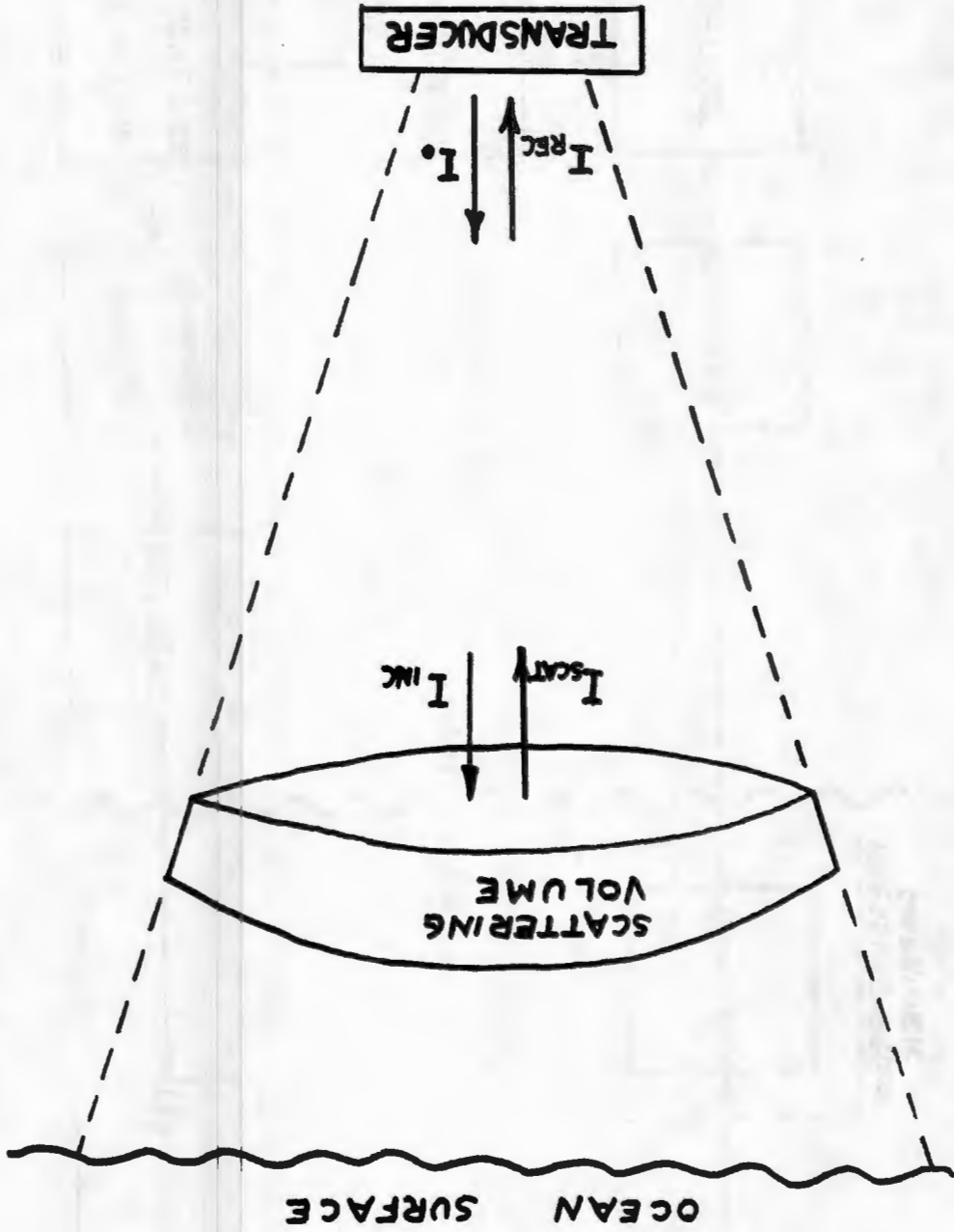
TABLE 3

REVERBERATION SUBSYSTEM COMPONENTS

Pulse Generator:	General Radio Company Unit Pulse Generator Type 1217B
Function Generator:	Hewlett Packard 3300A Function Generator
Tone Burst Accessory:	Hewlett Packard 3302A
Power Amplifier:	Hewlett Packard 467A Power Amplifier
TR Switch:	Appendix C
Transducer:	60 cm diameter Mylar Transducer
Receive Preamplifier:	NUS Model 2010-30 (30 dB gain)
Receive Amplifier:	Hewlett Packard 466A A.C. Amplifier
Reference Hydrophone:	1/4-inch Barium Titanate Pickup
Reference Preamplifier:	NUS Model 2010-30 (30 dB gain)
Reference Amplifier:	Hewlett Packard 466A A.C. Amplifier
Oscilloscope:	Tektronics Type 545 Oscilloscope
Polarizer:	Appendix C
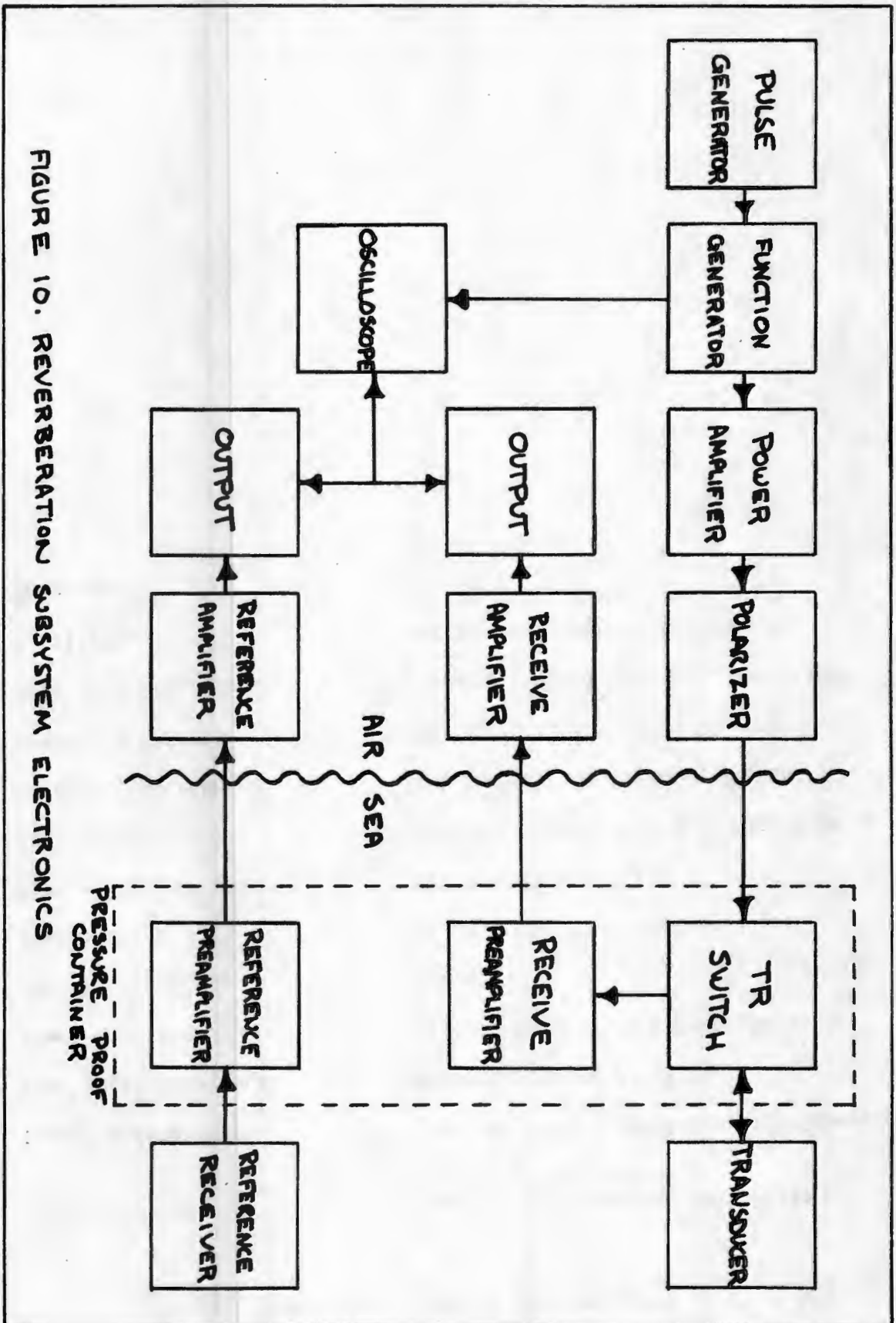
FIGURE 10. REVERBERATION SUBSYSTEM ELECTRONICS

REVERBERATION SUBSYSTEM

STANDING WAVE SUBSYSTEM

JAM CLEAT AND PULLEY

DEPTH CONTROL

RELEASE

ANCHOR
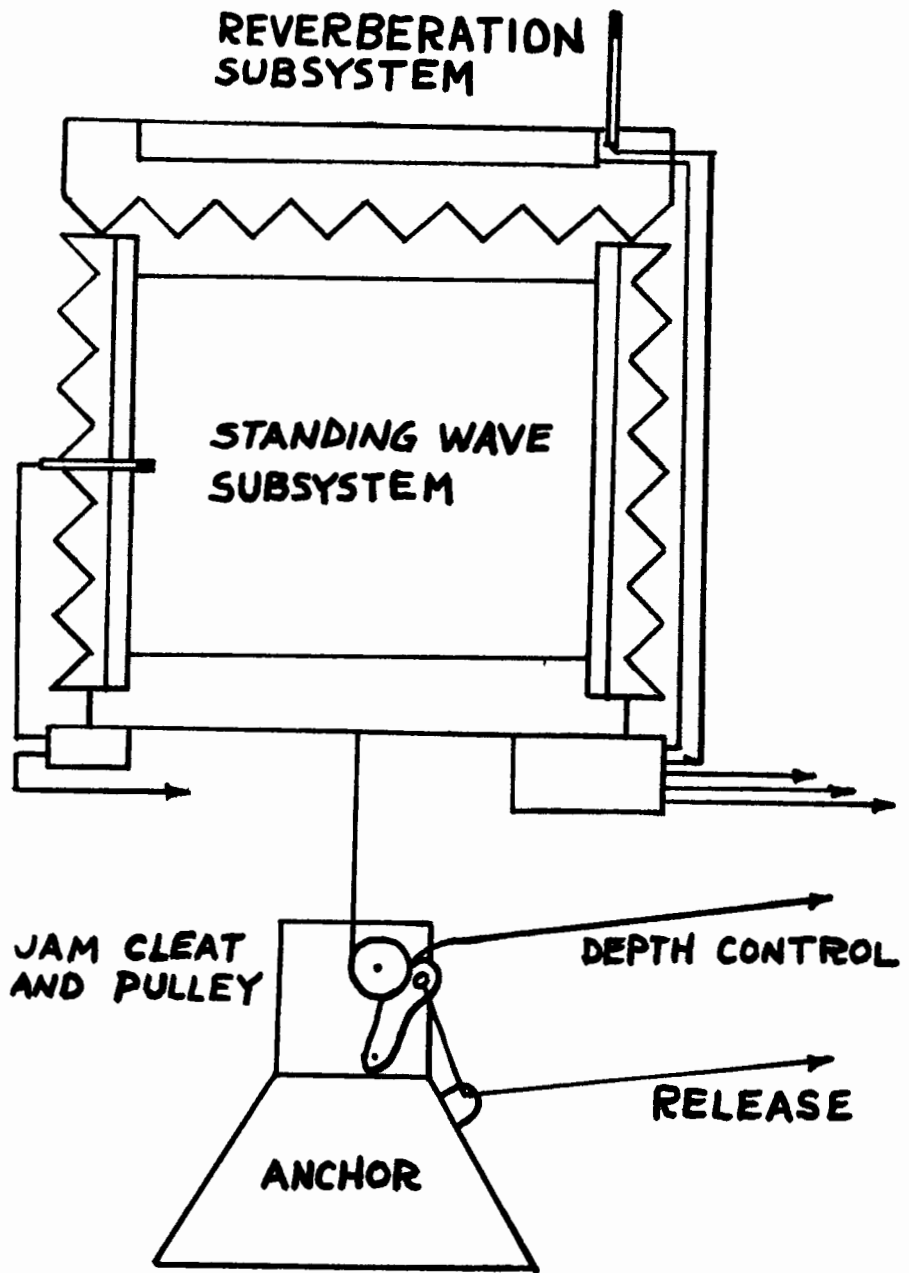
FIGURE II. COMPOSITE SYSTEM

REVERBERATION
CONTAINER

STANDING WAVE
CONTAINER

FIGURE 12. PRESSURE-PROOF CONTAINERS
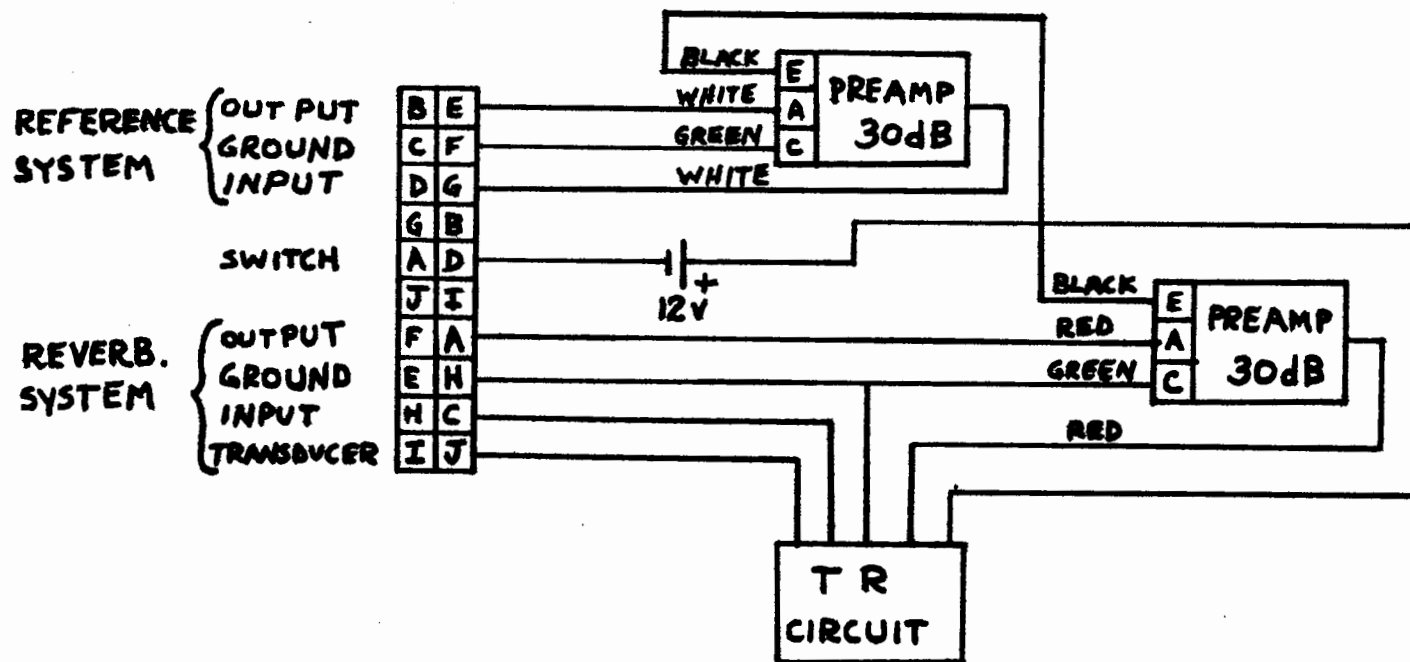
FIGURE 13. TRANSMIT-RECEIVE SWITCH
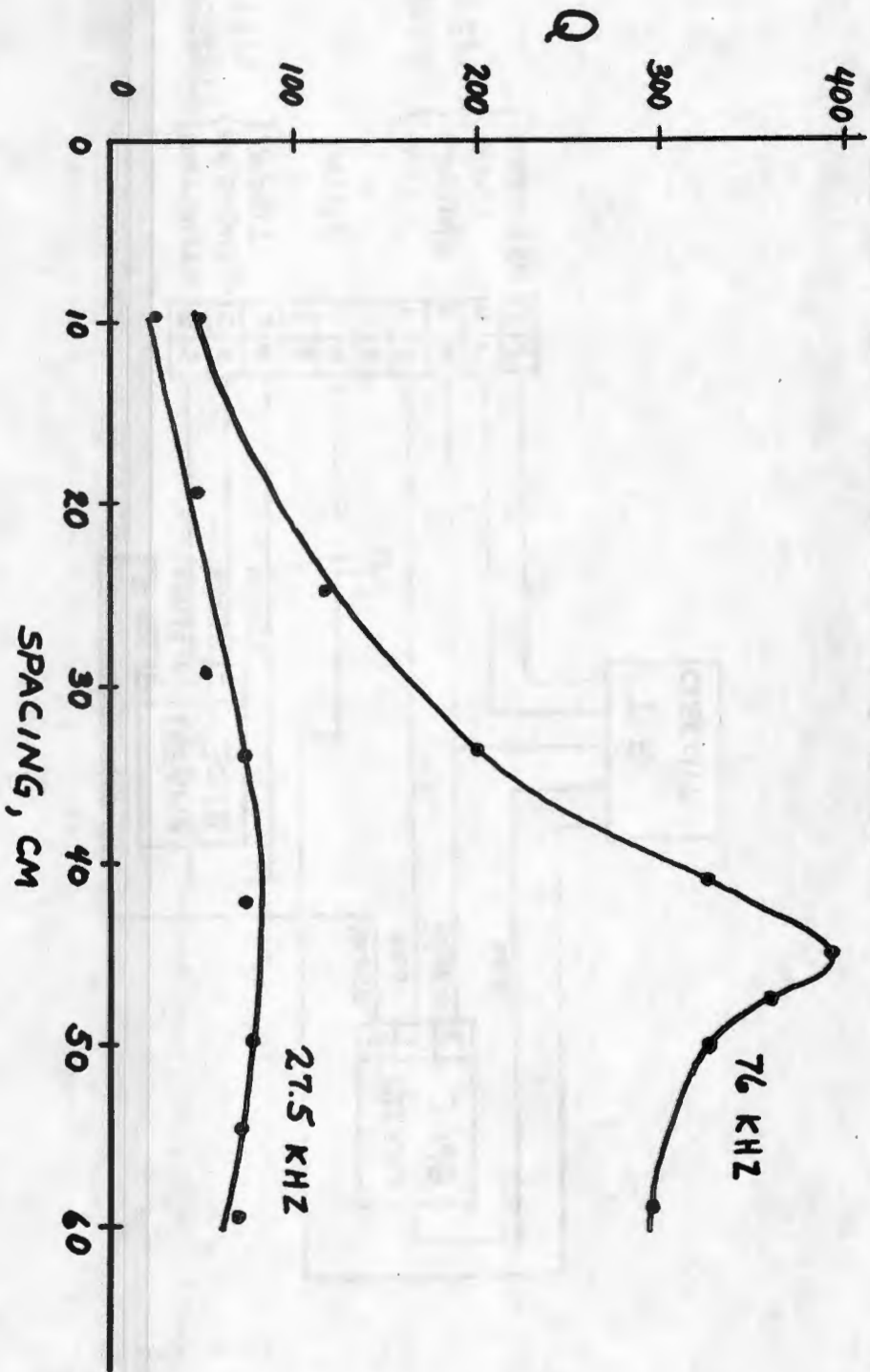
FIGURE 14. Q AS A FUNCTION OF SPACING AND FREQUENCY
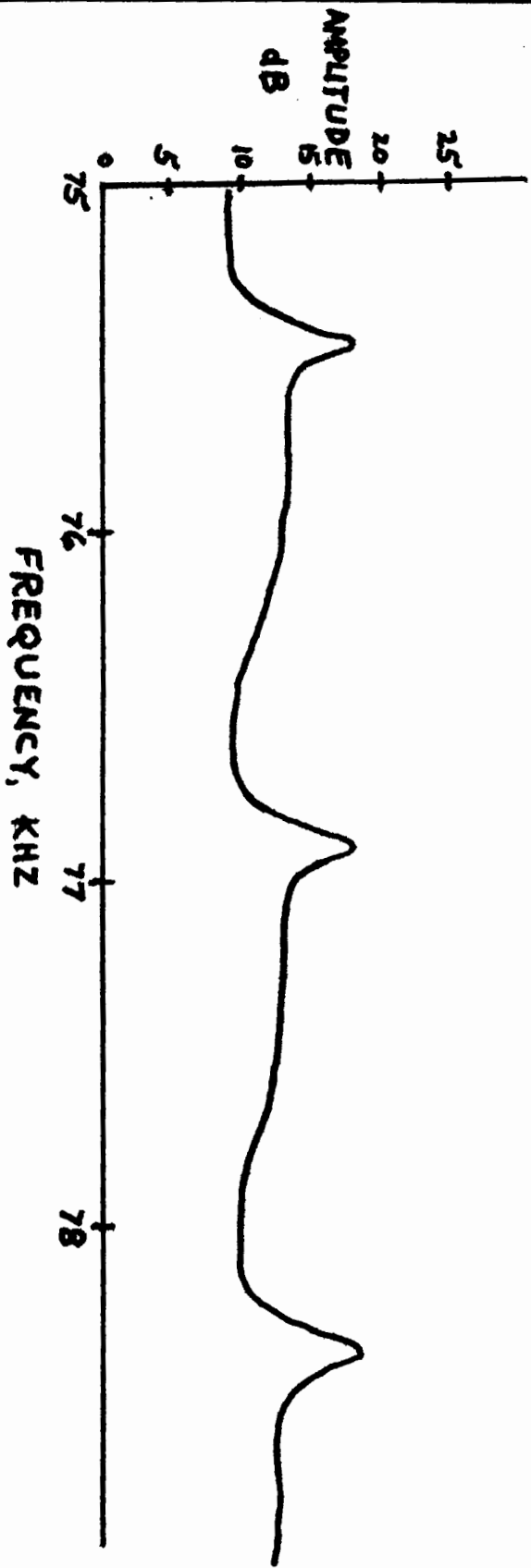
FIGURE 15. TYPICAL STANDING-WAVE Q CURVE

FIGURE 16. TYPICAL DIRECTIVITY PATTERN OF
REVERBERATION SUBSYSTEM TRANSDUCER
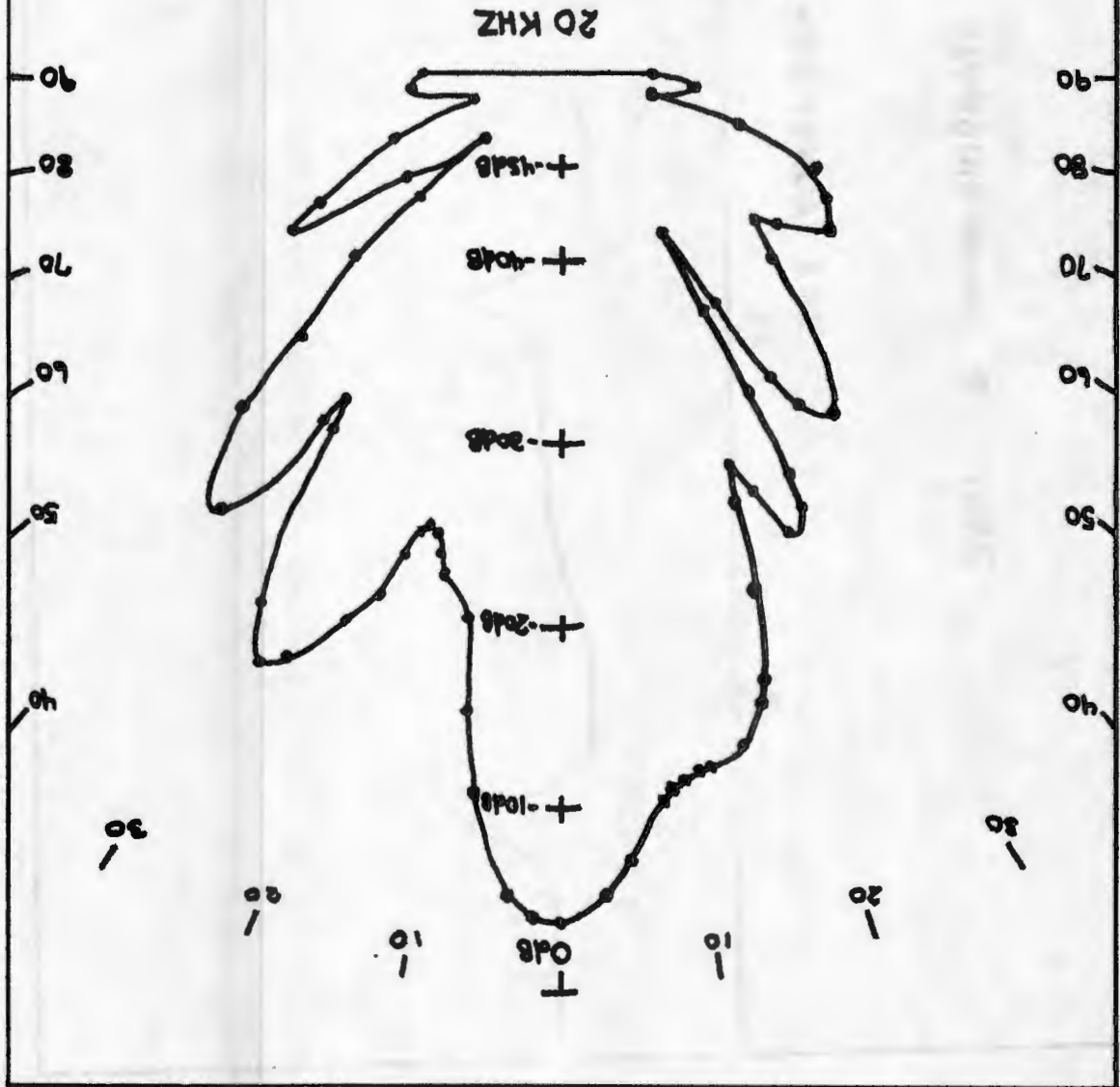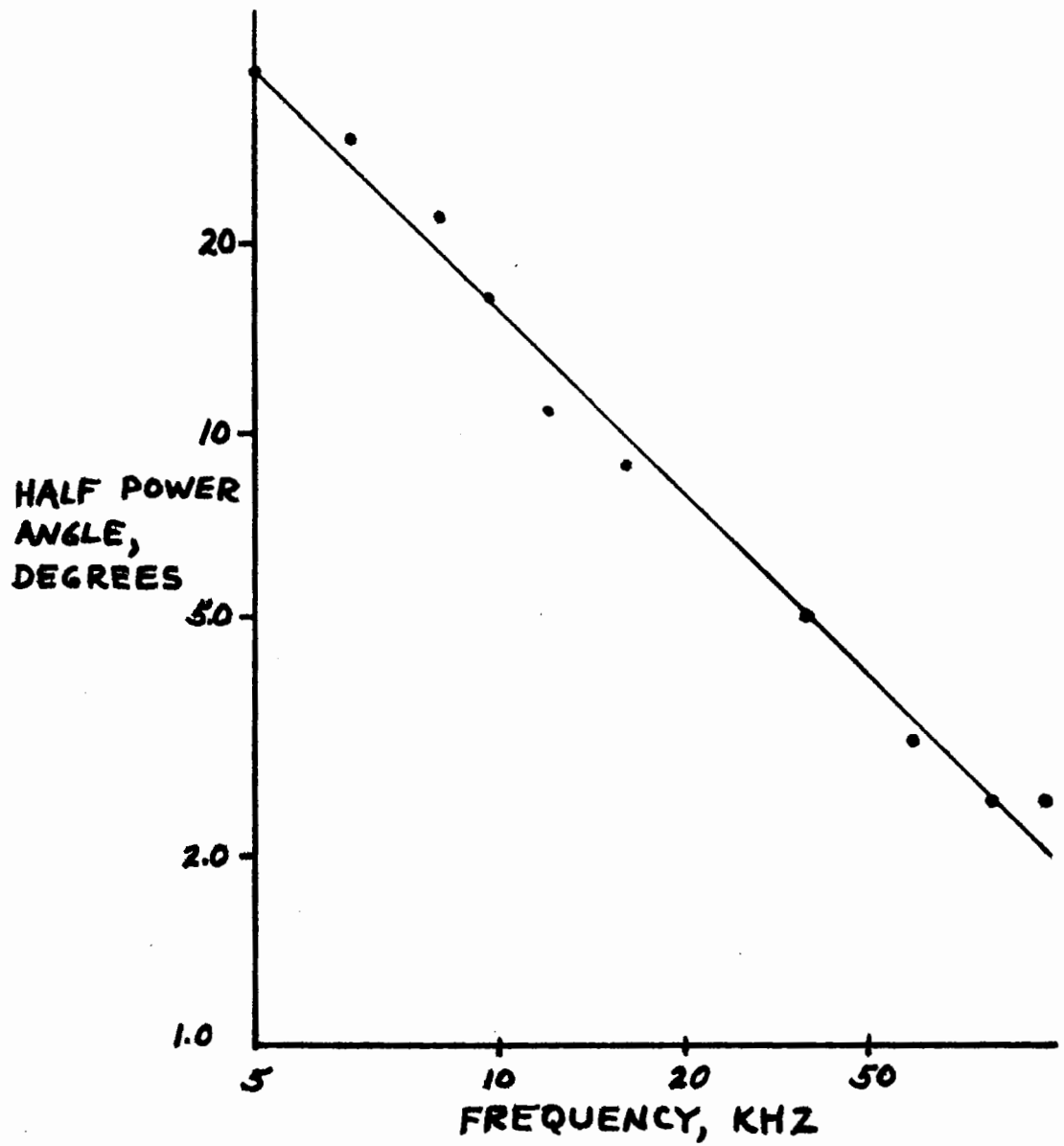
FIGURE 17. REVERBERATION TRANSDUCER
HALF-POWER ANGLE AS A FUNCTION OF
FREQUENCY
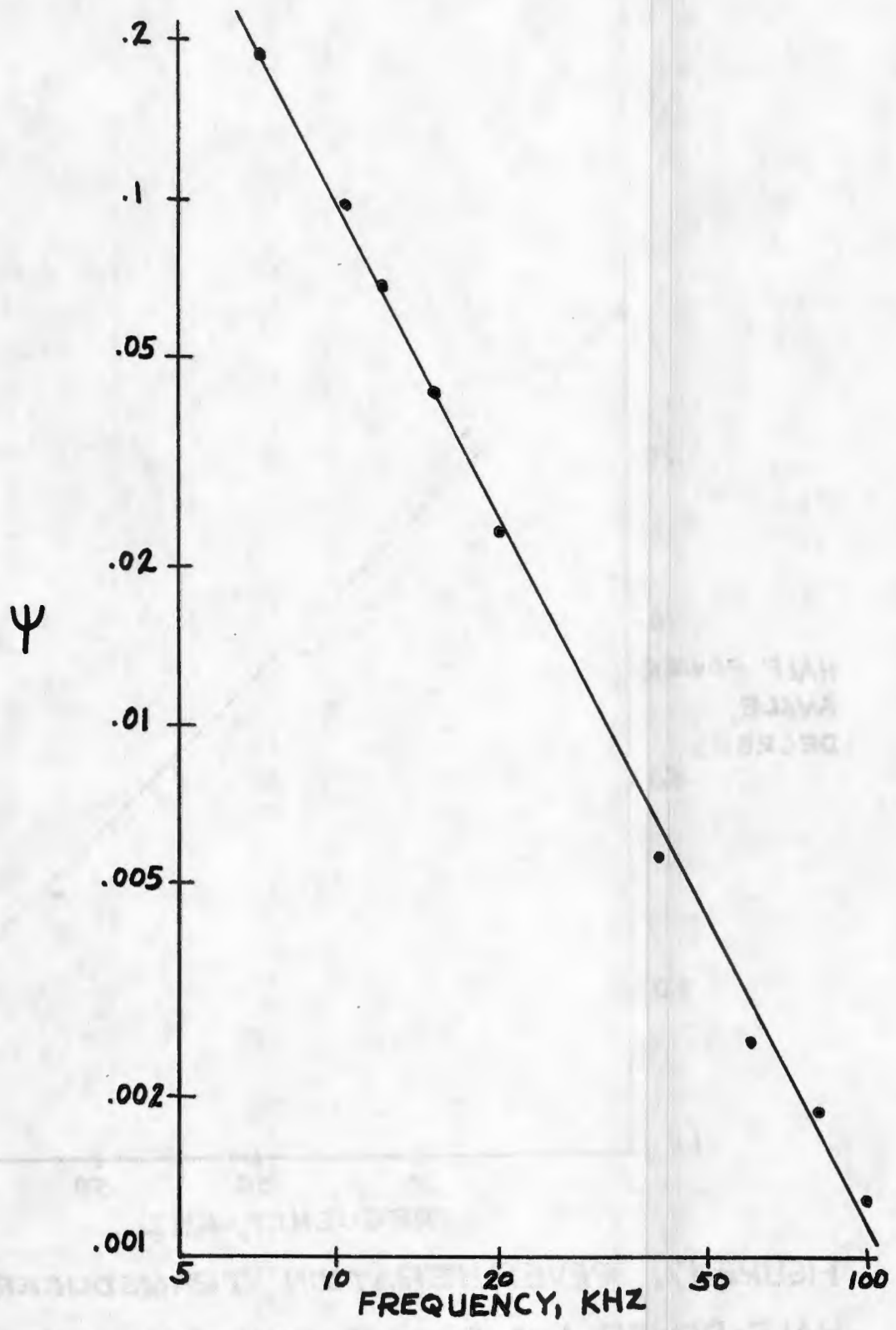
FIGURE 18. REVERBERATION TRANSDUCER ENSONIFIED
SOLID ANGLE AS A FUNCTION OF FREQUENCY
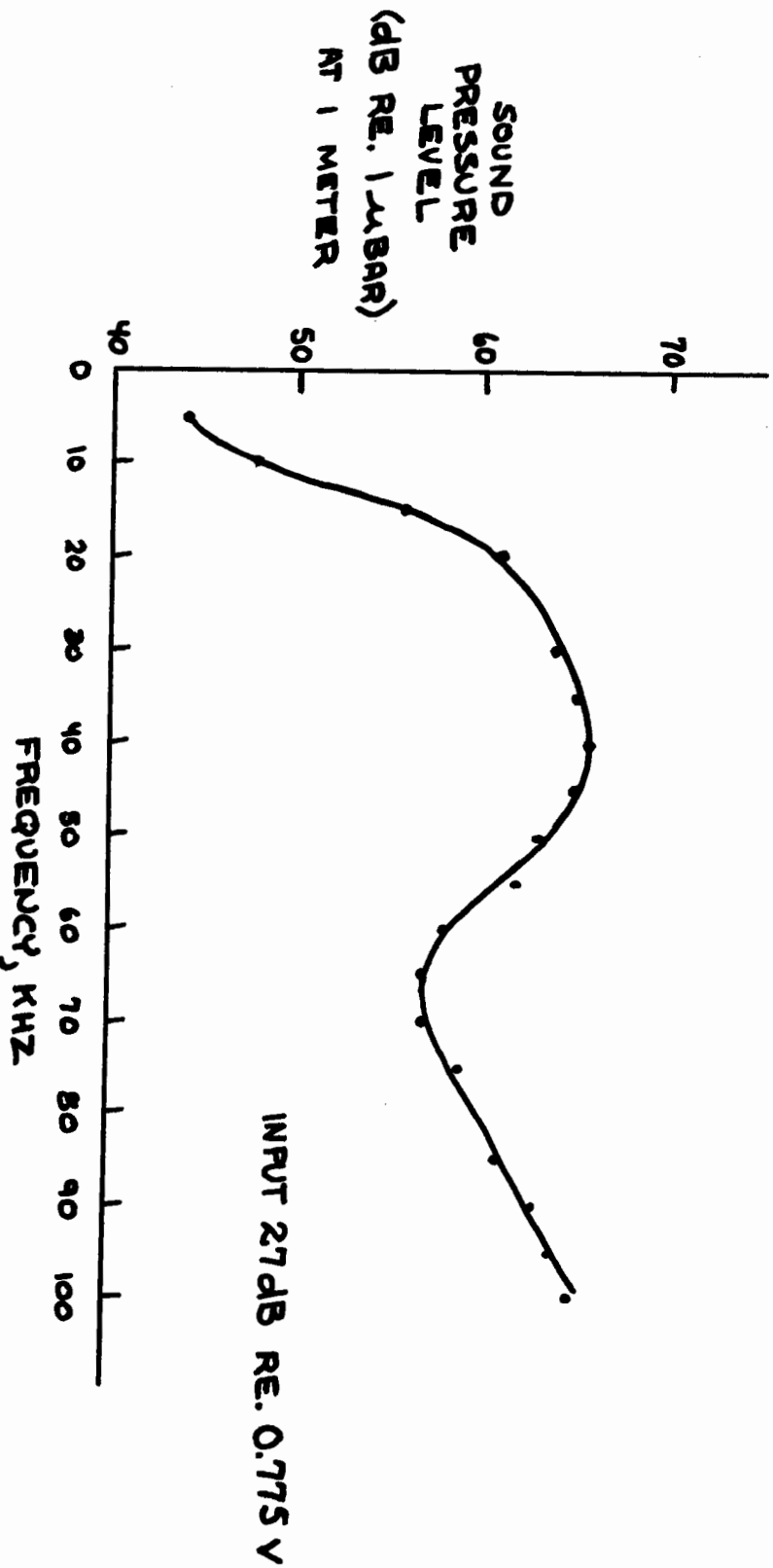
FIGURE 19. REVERBERATION TRANSDUCER SOUND PRESSURE LEVEL AS A FUNCTION OF FREQUENCY
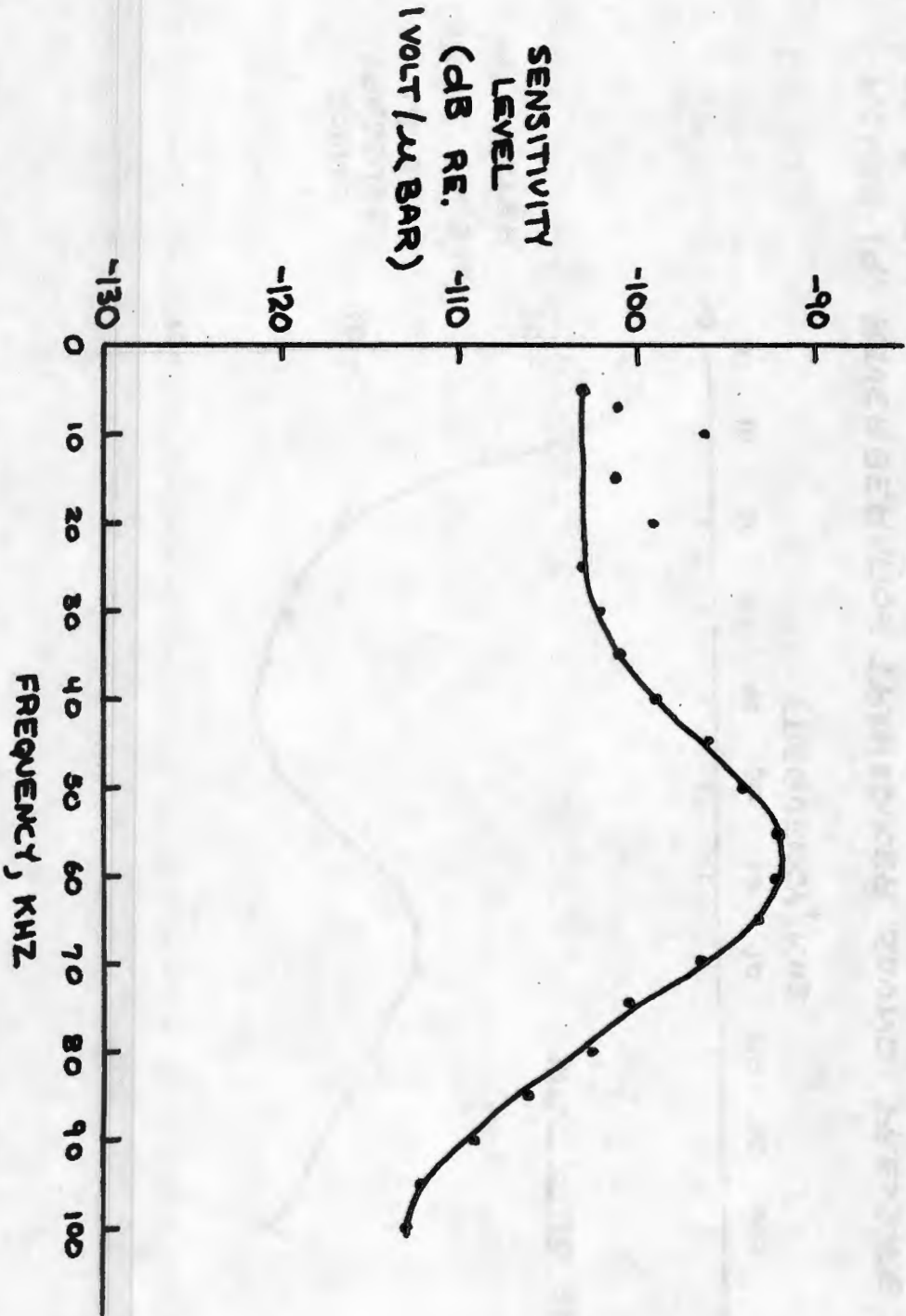
FIGURE 20. REVERBERATION TRANSDUCER SENSITIVITY LEVEL AS A
FUNCTION OF FREQUENCY
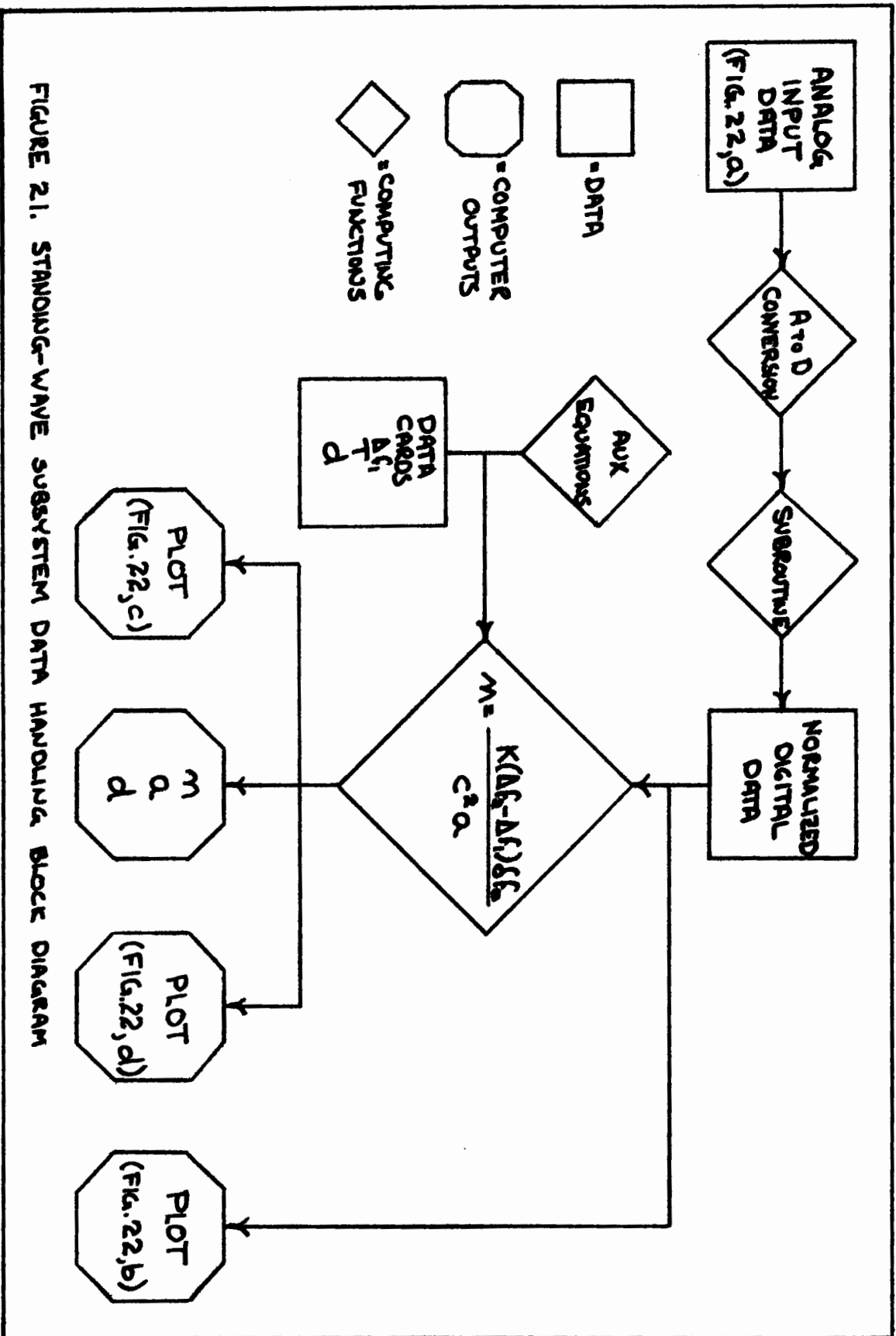
FIGURE 2.1. STANDING-WAVE SUBSYSTEM DATA HANDLING BLOCK DIAGRAM
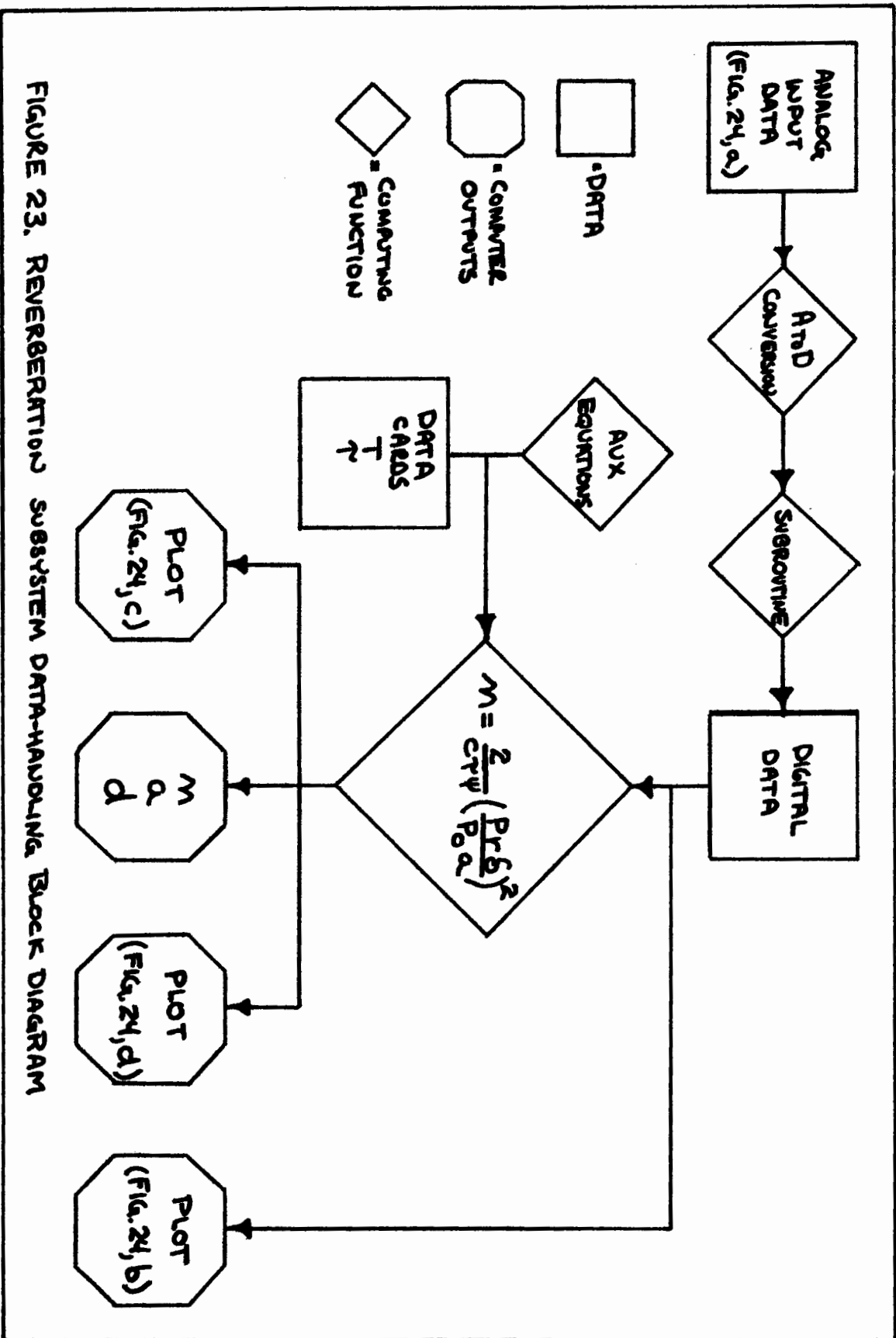
FIGURE 23. REVERBERATION SUBSYSTEM DATA-HANDLING BLOCK DIAGRAM

FIGURE 24. REPRESENTATION OF REVERBERATION DATA

(a) ANALOG INPUT DATA
(b) DIGITAL DATA
(c) BUBBLE CONCENTRATION AS A FUNCTION OF RADIUS
(d) BUBBLE CONCENTRATION AS A FUNCTION OF DEPTH

t = TIME, SEC
r = RANGE OF BUBBLES FROM TRANSDUCER, M
d = DEPTH OF BUBBLES, M
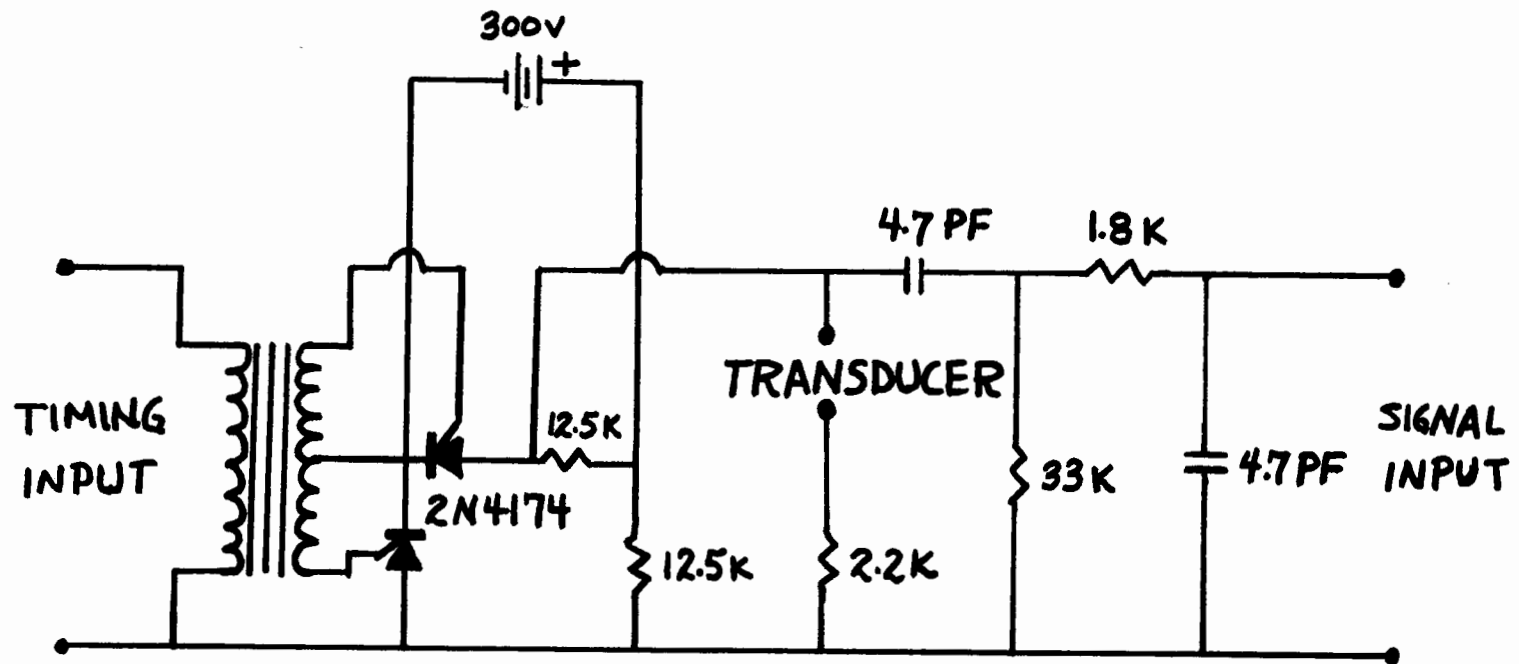m = BUBBLE CONCENTRATION, BUBBLES / M^3
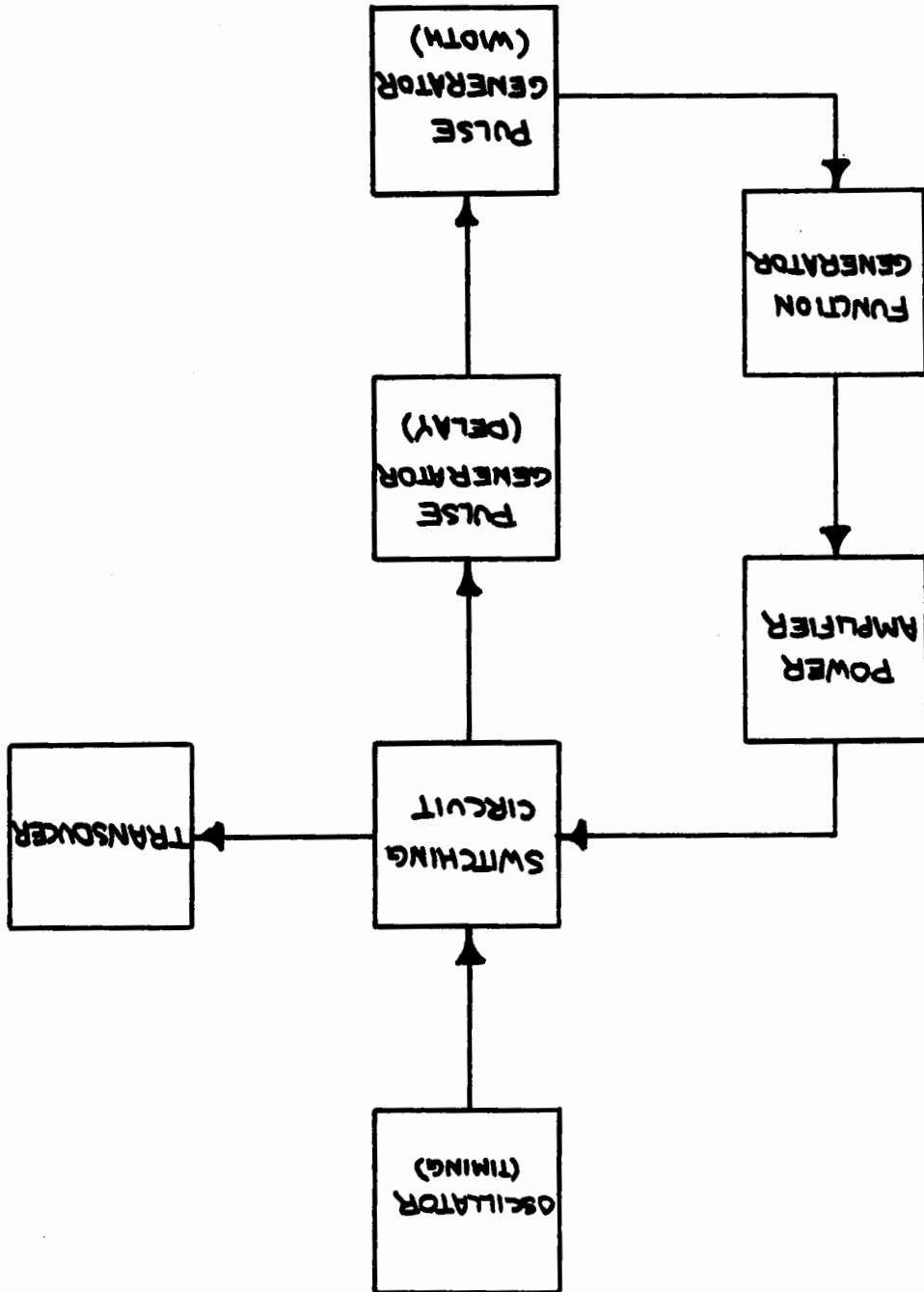a = BUBBLE RADIUS, MICRONS
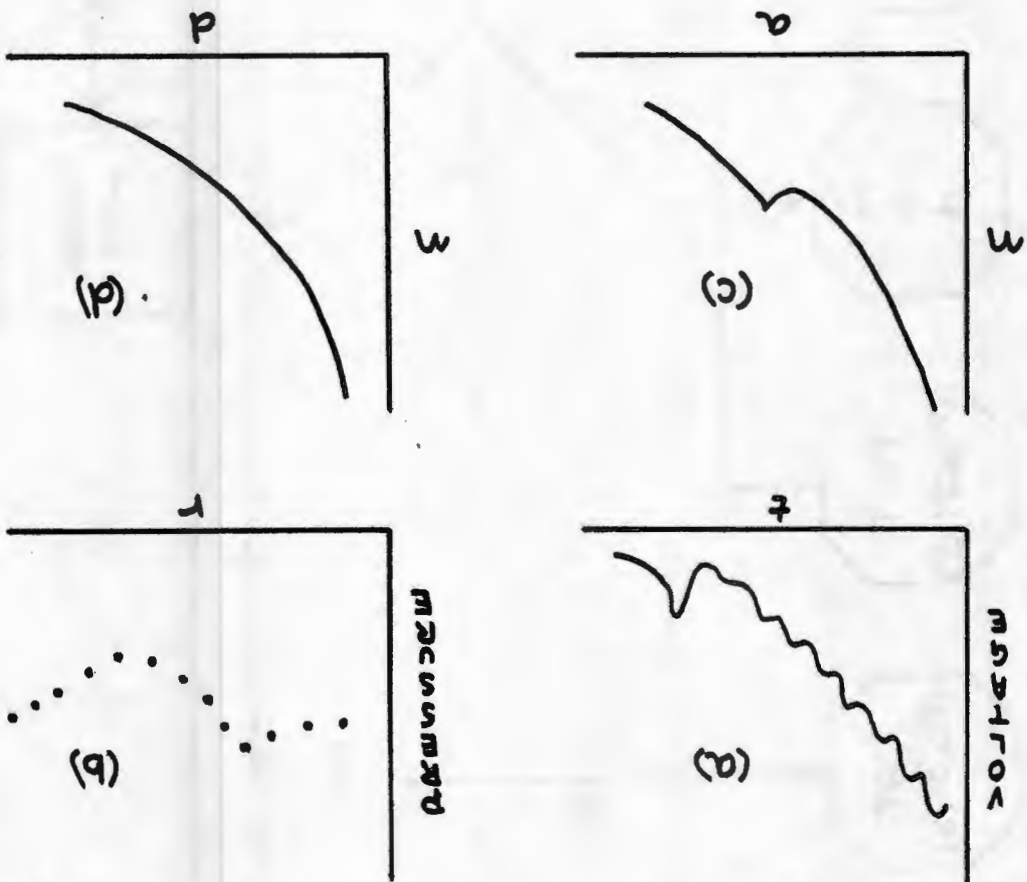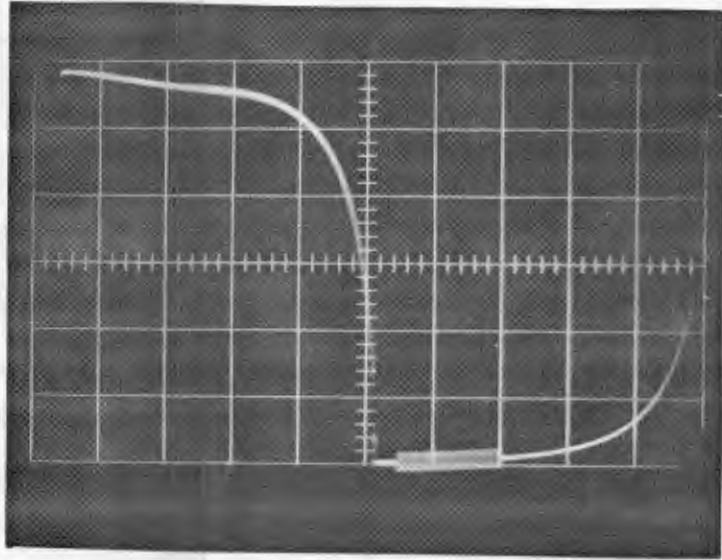
FIGURE 25. POLARIZATION NETWORK

TABLE 4

ALTERNATING-POLARIZATION NETWORK COMPONENTS

Oscillator:	Hewlett Packard 3300A Function Generator
Pulse Generators:	General Radio Company Unit Pulse Generator Type 1217B (2 required)
Function Generator:	Wavetek VCG Model 114
Power Amplifier:	Hewlett Packard 467A Power Amplifier
Transducer:	Mylar Transducer

PULSE GENERATOR (WIDTH)

FUNCTION GENERATOR

PULSE GENERATOR (DELAY)

POWER AMPLIFIER

TRANSDUCER

SWITCHING CIRCUIT

OSCILLATOR (TIMING)

FIGURE 26. ALTERNATING-POLARIZATION SYSTEM BLOCK DIAGRAM

TABLE 5

TRANSMIT-RECEIVE NETWORK COMPONENTS

Pulse Generator: General Radio Company Unit Pulse
                            Generator Type 1217B

Function Generator: Hewlett Packard 3300A Function Generator

Tone Burst Accessory: Hewlett Packard 3302A

Power Amplifier: Hewlett Packard 467A Power Amplifier

Preamplifier: NUS Model 2010-30 (30 dB gain)

Amplifier: Hewlett Packard 466A A.C. Amplifier

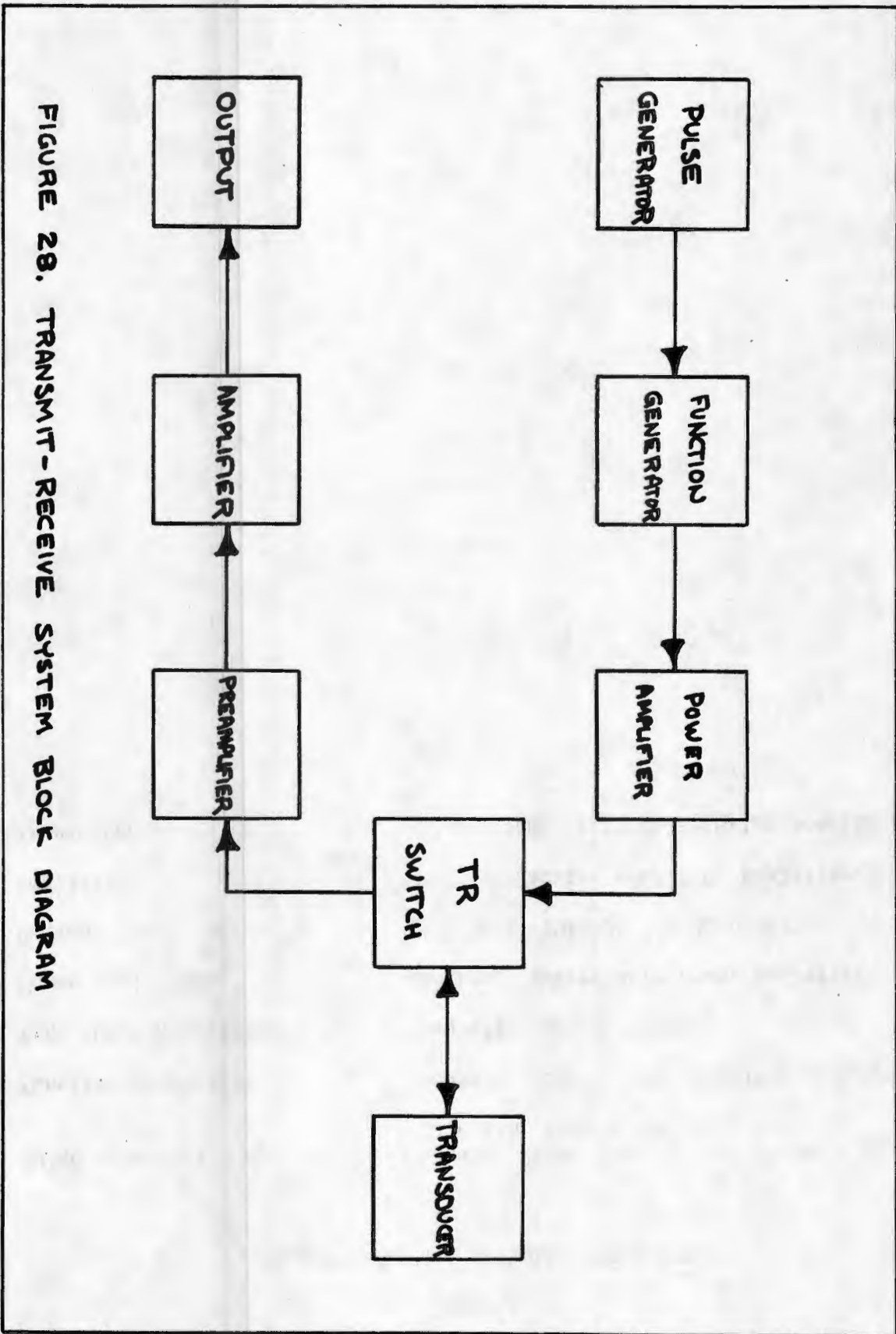Transducer: 60 cm diameter Circular Mylar Transducer
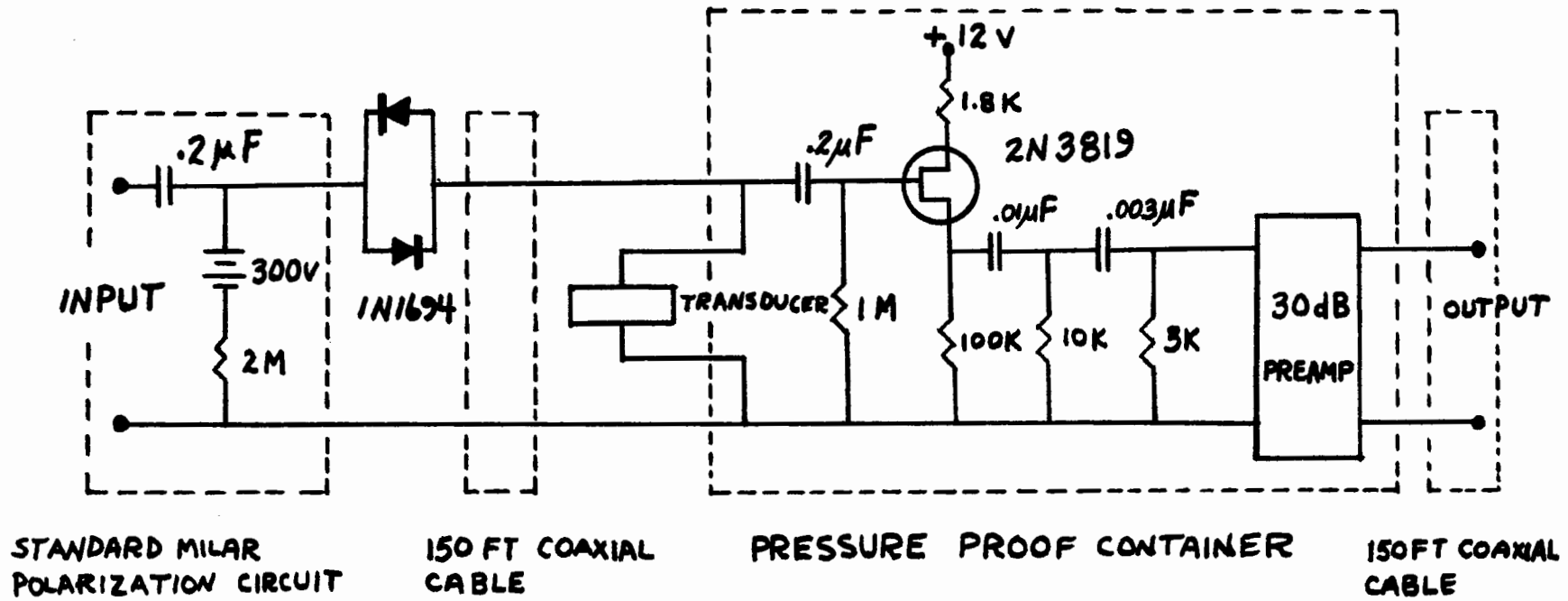
FIGURE 28. TRANSMIT-RECEIVE SYSTEM BLOCK DIAGRAM

FIGURE 29. TRANSMIT-RECEIVE CIRCUIT

73

A PULSED SIGNAL APPLIED TO A MYLAR TRANSDUCER IS SHOWN IN THE UPPER TRACE (5v/cm, 0.5ms/cm). THE PULSE IS PARTIALLY CLAMPED POSITIVE TO GROUND. A RECEIVED ECHO IS SHOWN IN THE LOWER TRACE (1V/cm, 0.5ms/cm).
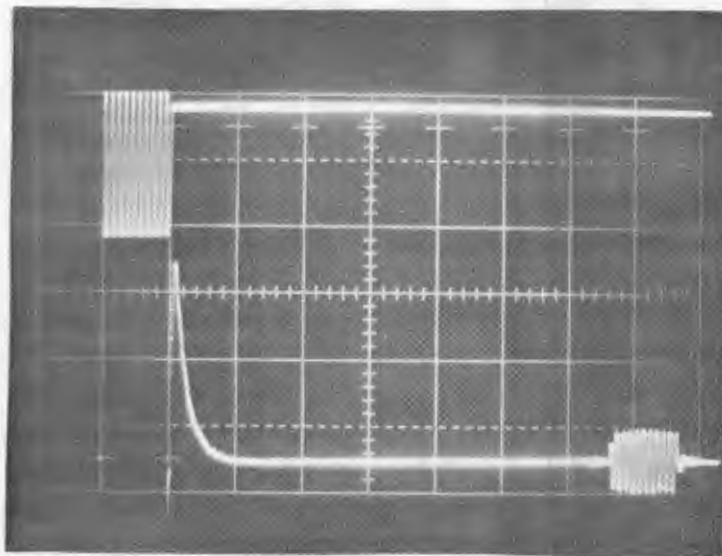

FIGURE 30. OSCILLOSCOPE PHOTOGRAPH OF OPERATING TRANSMIT-RECEIVE SYSTEM

COMPONENTS

[BUBBLE GENERATOR] ← [POWER AMPLIFIER] ← [FUNCTION GENERATOR]

FUNCTION GENERATOR: WAVETECH VCG MODEL 114
SETTINGS: SQUARE WAVE, 2.5 HZ
POWER AMPLIFIER: HEWLETT PACKARD 467 A
SETTINGS: 40 VOLTS OUTPUT

GENERATOR

INPUT

AIR
WATER

GROUND

NEOPRENE COATED ← 0.096 COPPER WIRE

0.020 → TUNGSTON WIRE

(NEOPRENE COATED EXCEPT FOR SMOOTHED TIPS)

FIGURE 31. BUBBLE GENERATOR
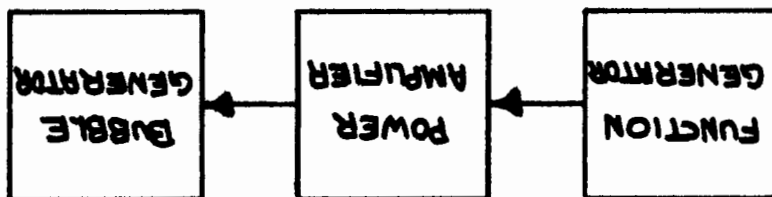
BIBLIOGRAPHY

1. Blanchard, D. C. and Woodcock, A. H., "Bubble Formation and Modification in the Sea and its Meteorological Significance," Tellus, V. 9, p. 145-158, September 1957.

2. Glotov, V. P., Kolobaev, P. A. and Neuimin, G. G., "Investigation of the Scattering of Sound by Bubbles Generated by an Artificial Wind in Sea Water and the Statistical Distribution of Bubble Sizes," Soviet Physics-Acoustics, V. 7, p. 341-345, April-June 1962.

3. Zimdar, R. E., Barnhouse, P. D., and Stoffel, M. J., Instrumentation to Determine the Presence and Acoustic Effect of Microbubbles Near the Sea Surface, Thesis, Naval Postgraduate School, Monterey, 1964.

4. Buxcey, S., McNeil, J. E., Marks, R. H. Jr, Acoustic Detection of Microbubbles and Particulate Matter Near the Sea Surface, Thesis, Naval Postgraduate School, Monterey, 1965.

5. Keller, D. G., Evaluation of a Standing Wave System for Determining the Presence and Acoustic Effect of Microbubbles Near the Sea Surface, Thesis, Naval Postgraduate School, Monterey, 1968.

6. NDRC Technical Reports, DIV. 6, V. 8, Part IV.

7. Devin, C., "Damping of Pulsating Air Bubbles in Water," JASA, V. 31, p. 1654, 1959.

8. Medwin, H., "In-Situ Acoustic Measurements of Bubble Populations in Coastal Ocean Waters," to be published in: Journal of Geophysical Research, 20 December 1969.

9. Bell Telephone System Monograph 2491, The Story of Q, by E. I. Geen.

10. Heuter, T. F. and Bolt, R. H., Sonics, Wiley, 1955.

11. Department of the Navy Military Specification for Vibration Damping Materials.

12. Urick, R. J., Principles of Underwater Sound for Engineers, McGraw-Hill, 1967.

13. Vennard, J. K., Elementary Fluid Mechanics, 4th Edition, Wiley, 1961.

14. Kinsler, L. E. and Frey, A. R., Fundamentals of Acoustics, 2nd Edition, Wiley, 1962.

INITIAL DISTRIBUTION LIST

No. Copies

1. Defense Documentation Center   20
   Cameron Station
   Alexandria, Virginia 22314

2. Library, Code 0212   2
   Naval Postgraduate School
   Monterey, California 93940

3. Commander, Naval Ordnance Systems Command   1
   Department of the Navy
   Washington, D. C. 20360

4. Professor H. Medwin, Code 61Md   10
   Department of Physics
   Naval Postgraduate School
   Monterey, Californa 93940

5. LT William J. Donaldson, USN   1
   USS Tirante (SS-420)
   FPO New York   09501

6. LCDR Byron N. Macfarlane, USN   1
   USS Haleakala (AE-25)
   FPO San Francisco   96601

7. Mr. William Smith   1
   Department of Physics
   Naval Postgraduate School
   Monterey, California 93940

8. Commander, Naval Ship Systems Command   1
   ATTN: Code 00V1K
   Department of the Navy
   Washington, D. C. 20305

9. Commander, Anti-Submarine Warfare Systems   1
   Projects Office
   Department of the Navy
   Washington, D. C. 20360

10. Commander, U. S. Naval Oceanographic Office   1
    Washington, D. C. 20390
    ATTN: Code 037-B

11. Director Acoustics Program (Code 468)   1
    Office of Naval Research, Navy Department
    Washington, D. C. 20360

77

DOCUMENT CONTROL DATA - R & D

(Security classification of title, body of abstract and indexing annotation must be entered when the overall report is classified)

1. ORIGINATING ACTIVITY *(Corporate author)*	2a. REPORT SECURITY CLASSIFICATION
Naval Postgraduate School Monterey, California 93940	Unclassified
	2b. GROUP

3. REPORT TITLE

Design of an Improved Acoustic System for Determination of the Concentration of Microbubbles in the Ocean

4. DESCRIPTIVE NOTES *(Type of report and inclusive dates)*

Master's Thesis; December 1969

5. AUTHOR(S) *(First name, middle initial, last name)*

William Jay Donaldson
Byron Noble Macfarlane

6. REPORT DATE	7a. TOTAL NO. OF PAGES	7b. NO. OF REFS
December 1969	77	14

8a. CONTRACT OR GRANT NO.	9a. ORIGINATOR'S REPORT NUMBER(S)
b. PROJECT NO.	
c.	9b. OTHER REPORT NO(S) *(Any other numbers that may be assigned this report)*
d.	

10. DISTRIBUTION STATEMENT

This document has been approved for public release and sale; its distribution is unlimited.

11. SUPPLEMENTARY NOTES	12. SPONSORING MILITARY ACTIVITY
	Naval Postgraduate School Monterey, California 93940

13. ABSTRACT

An acoustic system was designed to investigate microbubble concentrations and distributions in the ocean. The system consisted of a one-dimensional standing-wave resonator and a reverberation sensor. Concentrations are determined by measurement of the variation in system Q and the change in reverberation level produced by the resonant bubble response. The resonator and the sensor, while functioning independently, both measure bubble concentration as a function of depth and inferred size and thus provide a unique data comparison. The system has been designed to measure bubbles from approximately 700 microns to 30 microns utilizing frequencies from 5 to 100 kHz at depths to 100 ft. Initial tests utilizing a bubble generator in an anechoic tank have demonstrated the system's capability to measure bubble concentrations.

DD FORM 1 NOV 65 **1473** (PAGE 1)

S/N 0101-807-6811

A-31408

14. KEY WORDS	LINK A		LINK B		LINK C	
	ROLE	WT	ROLE	WT	ROLE	WT
Resonant						
Microbubbles						
Standing Wave						
Reverberation						
Acoustic						

DD FORM 1473 (BACK)
1 NOV 65

S/N 0101-807-6821

Security Classification

A-31409